N70-24253

NASA TECHNICAL MEMORANDUM

NASA TM X-1996

NASA TM X-1996

CASE FILE COPY

LOW-SUBSONIC AERODYNAMIC CHARACTERISTICS OF A MODEL OF A FIXED-WING SPACE SHUTTLE CONCEPT AT ANGLES OF ATTACK TO 76°

by John P. Decker and Bernard Spencer, Jr.

Langley Research Center
Langley Station, Hampton, Va.

NATIONAL AERONAUTICS AND SPACE ADMINISTRATION • WASHINGTON, D. C. • APRIL 1970

1. Report No. NASA TM X-1996	2. Government Accession No.	3. Recipient's Catalog No.
4. Title and Subtitle LOW-SUBSONIC AERODYNAMIC CHARACTERISTICS OF A MODEL OF A FIXED-WING SPACE SHUTTLE CONCEPT AT ANGLES OF ATTACK TO 76^{0}		5. Report Date April 1970
		6. Performing Organization Code
7. Author(s) John P. Decker and Bernard Spencer, Jr.		8. Performing Organization Report No. L-6985
		10. Work Unit No. 124-64-01-06-23
9. Performing Organization Name and Address NASA Langley Research Center Hampton, Va. 23365		11. Contract or Grant No.
		13. Type of Report and Period Covered Technical Memorandum
12. Sponsoring Agency Name and Address National Aeronautics and Space Administration Washington, D.C. 20546		14. Sponsoring Agency Code

15. Supplementary Notes

16. Abstract

An investigation was conducted in the Langley low-turbulence pressure tunnel on a model of the second stage (orbiter) of the two-stage space shuttle concept proposed by the NASA Manned Spacecraft Center. The tests were conducted at angles of attack from about -7^{0} to 76^{0} to examine the subsonic pitch-down maneuver from high to low angles as well as to obtain some basic stability and control data at low angles of attack. The two-stage launch configuration was simulated for testing when the basic orbiter model was assumed to represent the first stage and a scaled second stage was placed in a "piggyback" fashion in the approximate location as conceptually proposed. The tests were conducted at a Mach number of approximately 0.25 at Reynolds numbers per foot from about 1.7×10^{6} to 12.3×10^{6} (per meter from about 5.6×10^{6} to 40.4×10^{6}).

17. Key Words Suggested by Author(s) Space shuttle	18. Distribution Statement Unclassified – Unlimited

19. Security Classif. (of this report)	20. Security Classif. (of this page)	21. No. of Pages	22. Price*
Unclassified	Unclassified	52	$3.00

*For sale by the Clearinghouse for Federal Scientific and Technical Information
Springfield, Virginia 22151

LOW-SUBSONIC AERODYNAMIC CHARACTERISTICS OF A MODEL OF A FIXED-WING SPACE SHUTTLE CONCEPT AT ANGLES OF ATTACK TO 76°

By John P. Decker and Bernard Spencer, Jr.
Langley Research Center

SUMMARY

An investigation was conducted in the Langley low-turbulence pressure tunnel on a model of the second stage (orbiter) of the two-stage space shuttle concept proposed by the NASA Manned Spacecraft Center. The tests were conducted at angles of attack from about -7° to 76° to examine the subsonic pitch-down maneuver from high to low angles, as well as to obtain some basic stability and control data at low angles of attack. The two-stage launch configuration was simulated for testing when the basic orbiter model was assumed to represent the first stage and a scaled second stage was placed in a "piggyback" fashion in the approximate location as conceptually proposed. The tests were conducted at a Mach number of approximately 0.25 at Reynolds numbers per foot from about 1.7×10^6 to 12.3×10^6 (per meter from about 5.6×10^6 to 40.4×10^6).

Results of the investigation indicate that the configuration is Reynolds number sensitive; for example, with increasing Reynolds number, the maximum untrimmed lift-drag ratio increased from 7.2 to 8.6 and the longitudinal stability decreased at low angles of attack. The original proposed configuration was longitudinally unstable and just increasing horizontal-tail size to 1.70 of the original tail size was insufficient; positive stability was obtained when the leading-edge sweep of the horizontal tail was reduced from 70° to 41° with a simultaneous change in the planform shape from delta to clipped delta and, consequently, an area increase to 2.20 times the size of the original tail. Positive longitudinal control was measured for elevator deflections up to ±20° at low angles of attack, but the trailing-edge elevator was completely ineffective at very high angles of attack. Addition of the upper stage to form a complete launch configuration shifted the center of pressure from about 43 percent to 56 percent of the basic body length forward of the base of the fuselage. The complete configuration indicated positive effective dihedral at angles of attack up to about 16° and was directionally stable at angles of attack up to about 10°.

INTRODUCTION

Whereas both the NASA and industry have studied the application of manned lifting bodies as reusable logistics vehicles (see refs. 1 and 2), considerable interest is at present focused on advanced reusable earth-orbital transportation systems capable of carrying exceptionally large payloads from and to earth. The spectrum of concepts envisioned at present encompass configurations from lifting-body-type first and second stages, such as the HL-10 concept and three identical (Trimese) stages having variable-geometry wings for landing, to a configuration of fixed high-aspect-ratio wing and conventional horizontal tail not dissimilar to present-day jet transports in both planform and size. All these concepts as presently envisioned would be rocket powered during ascent and may or may not have conventional air-breathing engines for return to base and/or landing-field go-around capability. The present paper presents a preliminary static wind-tunnel study of the low-speed aerodynamic characteristics of one such conceptual design of the fixed-wing class previously mentioned. This concept, proposed by the NASA Manned Spacecraft Center, is a two-stage all-reusable system (orbiter plus booster) having horizontal-landing capability. The envisioned entry attitude for both the booster and orbiter vehicles (which are geometrically similar) is considered to occur at an angle of attack of approximately 60°, with this attitude maintained until low-subsonic Mach numbers are achieved. The vehicle is then considered to be rotated by means of aerodynamic controls to attitudes suitable for landing (i.e., angles of attack from about 8° to 16°).

The vehicle design for both stages consists of a flat-bottom lifting body, fixed wing of moderate aspect ratio, and conventional horizontal tail. The body is highly blunted, with a modified rectangular cross section. The wing has an aspect ratio of 7.0, moderate thickness ratio, and leading-edge sweep of 14°. Longitudinal stability and control are provided by a horizontal tail, and lateral-directional stability is provided by a single center vertical tail. Flyback capability is obtained with turbojet engines mounted on the wing upper surface.

The present investigation was conducted in the Langley low-turbulence pressure tunnel on a model of the second stage (orbiter) of the two-stage space shuttle concept. The tests were conducted at angles of attack from about -7° to 76° to examine the subsonic pitch-down maneuver from high to low angles as well as to obtain the effects of Reynolds number and some basic stability and control data at low angles of attack. The two-stage launch configuration was simulated for testing when the basic orbiter model was assumed to represent the first stage and a scaled second stage was placed in a "piggyback" fashion in the approximate location as conceptually proposed. The tests were conducted at a Mach number of approximately 0.25 at Reynolds numbers per foot from about 1.7×10^{6} to 12.3×10^{6} (per meter from about 5.6×10^{6} to 40.4×10^{6}).

SYMBOLS

The data of the present investigation are referred to the body-axis system except the lift and drag coefficients, which are referred to the stability-axis system. The estimated center of gravity was located at 11.89 in. (30.20 cm) from the base of the fuselage. All coefficients are based on the total planform area, mean geometric chord, and span of the wing.

b wing span, 18.00 in. (45.72 cm)

$\bar{c}$ wing mean geometric chord, 2.78 in. (7.06 cm)

C_D drag coefficient, $\frac{\text{Drag}}{qS}$

C_L lift coefficient, $\frac{\text{Lift}}{qS}$

C_l rolling-moment coefficient, $\frac{\text{Rolling moment}}{qSb}$

C_{l_β} rolling-moment parameter, $\frac{\Delta C_l}{\Delta \beta}$

C_m pitching-moment coefficient, $\frac{\text{Pitching moment}}{qS\bar{c}}$

$C_{m_{\delta_e}}$ control effectiveness parameter, $\frac{\Delta C_m}{\Delta \delta_e}$

C_n yawing-moment coefficient, $\frac{\text{Yawing moment}}{qSb}$

C_{n_β} yawing-moment parameter, $\frac{\Delta C_n}{\Delta \beta}$

C_Y side-force coefficient, $\frac{\text{Side force}}{qS}$

C_{Y_β} side-force parameter, $\frac{\Delta C_Y}{\Delta \beta}$

l_9 length of body with 9° nose ramp angle, in. (cm)

L/D lift-drag ratio

q free-stream dynamic pressure

R Reynolds number

S reference wing area, 0.320 ft^2 (0.030 m^2)

x_{cp} location of center of pressure forward of base, in. (cm)

α angle of attack referred to body reference plane, deg

β angle of sideslip, deg

δ_e elevator deflection (positive for trailing edge down), deg

Model component designations:

B_9 body with 9° nose ramp angle

B_{20} body with 20° nose ramp angle

H_1 small horizontal 70° delta tail

H_2 large horizontal 70° delta tail

H_3 large horizontal 41° clipped delta tail

W wing

V vertical tail

DESCRIPTION OF MODEL

The vehicle tested was an approximate 0.02-scale model of the second stage (orbiter) of a two-stage space-shuttle-vehicle concept conceived at the NASA Manned Spacecraft Center. Details of the orbiter are shown in figure 1(a) and the general arrangement of the launch configuration is shown in figure 1(b). Geometric characteristics are presented in table I. Photographs of the model installed in the Langley low-turbulence pressure tunnel are presented as figure 2.

The fuselage, which was flat bottomed and highly blunted, had a modified rectangular cross section with a semicircular top and a hard chine leading edge. Some afterbody boattailing in the lateral plane was also included. Two nose ramp angles (9° and 20°) were considered. The wing was fixed in a low position with 4° of positive incidence relative to the body reference plane. The airfoil section varied from an NACA 0014-64 at the root chord to an NACA 0010-64 at the tip chord. The wing had a leading-edge sweep of 14°, taper ratio of 0.333, and aspect ratio of 7.0.

The originally proposed horizontal tail (designated H_1) had a 70° delta planform with a ratio of exposed tail area to total wing planform area of 0.235. A larger 70° delta tail (designated H_2), identical in planform shape to H_1, was also tested. The exposed tail area of H_2 was 1.70 times that of H_1. A 41° clipped delta tail (designated H_3) was also investigated. This tail was constrained to have the same root chord and trailing-edge location as H_1, as low a leading-edge sweep as feasible, and about one-third more area than H_2. The exposed area of H_3 was 2.20 times that of H_1. These tail variations were used to investigate the potential longitudinal-stability improvements that could be obtained by increasing tail area and reducing leading-edge sweep. The large 70° delta tail H_2 was provided with an elevator to obtain some preliminary control-effectiveness data. Elevator hinge line was coincident with the body base, and deflections from -60° to 60° were used.

The two-stage launch configuration was simulated for testing when the basic orbiter model was assumed to represent the first stage and a scaled second stage was placed in a "piggyback" fashion in the approximate longitudinal and vertical location as conceptually proposed. (See fig. 1(b).)

APPARATUS AND METHODS

Tunnel

The tests were conducted in the Langley low-turbulence pressure tunnel which is a variable-pressure, single-return facility having a closed test section which is 3.5 feet (1.1 meters) wide by 7 feet (2.1 meters) high. The tunnel can accommodate tests in air at Reynolds numbers per foot from approximately 1.0×10^6 to 15.0×10^6 (per meter from 3.3×10^6 to 49.2×10^6) at Mach numbers up to about 0.40.

Test Conditions

The major portion of the tests were conducted at a Mach number of approximately 0.25 at Reynolds numbers per foot from 1.7×10^6 to 12.3×10^6 (per meter from 5.6×10^6 to 40.4×10^6). The angle of attack was varied from about -7° to 76° for a sideslip angle

of 0°. Some tests were also made at a sideslip angle of 5° in the angle-of-attack range from about -7° to 20°. Most of the configurations were tested without transition strips. However, the effects of fixing transition were investigated by using a 0.05-inch-wide (0.12 cm) band of No. 80 carborundum grit located 1.20 inches (3.05 cm) behind the apex of the nose and horizontal-tail leading edge and at a distance behind the wing leading edge which varied from 0.80 inch (2.03 cm) at the wing-fuselage junction to 0.30 inch (0.76 cm) at the wing tip. These strips were located according to the methods described in reference 3.

Measurements and Corrections

The drag coefficients presented represent gross drag in that base drag has not been subtracted out. No blockage or lift-interference corrections have been applied to the data, but previous experience with models of similar size has indicated that such corrections would be negligible. Angles of attack have been corrected for balance and sting deflection due to aerodynamic load. Sideslip angles have not been corrected; these corrections would be of the order of 0.1° and therefore are considered insignificant.

PRESENTATION OF RESULTS

The results of this investigation are presented in the following figures:

DISCUSSION

Because of the preliminary nature of the configuration investigated no detailed analysis of the results is presented. Several areas of apparent aerodynamic interest are briefly discussed.

Longitudinal Aerodynamic Characteristics

Effect of transition.- The results of fixing transition on the B_9WH_2V configuration (fig. 3) indicate little or no effect on the drag or L/D characteristics of the vehicle and only minor effects on the lift and pitching-moment displacement. For this reason the remainder of the tests were run transition free.

Fuselage ramp angle.- For the fuselage with either the 9° or 20° nose ramp angle, the same static longitudinal stability was obtained at low angles of attack (fig. 4) and the aerodynamic center for each was located approximately 5 percent of the respective body length aft of the nose.

Effect of Reynolds number.- Figure 5 indicates that increasing the R/ft from 1.7×10^6 to 12.3×10^6 (R/m from 5.6×10^6 to 40.4×10^6) for a complete configuration (B_9WH_3V) at angles of attack up to 21° decreased the low-lift longitudinal stability and increased the angle of attack for the onset of flow separation on the wings from about 8° to 13° as evidenced by the plots of C_L against α and C_m against C_L. Increasing R/ft from 1.7×10^6 to 5.3×10^6 (R/m from 5.6×10^6 to 17.4×10^6) increased the maximum untrimmed L/D from 7.2 to 8.6. Further increases in the Reynolds number indicate only slight improvement in the maximum untrimmed L/D. Similar trends are also shown in figures 6 and 7 for B_9WV and B_9WH_2V, respectively, tested at angles of attack to about 76°. At angles of attack greater than about 36° there are significantly large changes in the magnitudes and variations of both C_L and C_m with angle of attack resulting from increasing Reynolds number.

Effect of horizontal tail.- The effects of horizontal-tail size and geometry are presented in figures 8, 9, and 10 and indicate that the complete configuration having either 70° delta tail (H_1 or H_2) was longitudinally unstable at the lower angles of attack (see

fig. 8). This is primarily due to the extreme forward location of the aerodynamic center at low angles of attack for the body alone as previously mentioned. Increasing the horizontal-tail area to 2.20 of the area of H_1 and changing the tail geometry from a 70° delta tail (H_1 or H_2) to a 41° clipped delta tail (H_3) provided the configuration with static longitudinal stability at low angles of attack. (See figs. 8, 9, and 10.) In addition, the 41° clipped delta tail decreased the large positive C_m noted for H_1 or H_2 that must be overcome in order to trim the vehicle at angles of attack near 60°. (See fig. 9.)

Longitudinal control.- The effects of elevator deflection for horizontal tail H_2 are presented in figures 11 to 14 for two Reynolds numbers. At low angles of attack, the elevator was effective in producing negative or positive pitching-moment increments for deflections up to about 20° or -20°, respectively. (See figs. 11 to 14.) At elevator deflections greater than about 20° considerable loss in $C_{m_{\delta_e}}$ is noted as a result of flow separation existing on the tail. At angles of attack greater than about 62°, the elevator is completely ineffective for positive deflections and, consequently, the elevator will not trim the configuration at the highest test angles of attack. For negative deflections, the elevator provides some degree of effectiveness for deflections up to about -40°; however, a similar loss in $C_{m_{\delta_e}}$ is noted above $\delta_e = -20^{\circ}$. (See figs. 13 and 14.)

Effect of upper stage addition to simulate the launch configuration.- The addition of a scaled second stage to the basic orbiter model (B_9WH_2V) to simulate the launch configuration (fig. 17) moved the center of pressure at low angles of attack from about 43 percent to 56 percent of the body length forward of the base. For the basic orbiter model, the center of pressure moves forward with increasing angle of attack, which is destabilizing effect. For the simulated launch configuration, the center of pressure moves slightly rearward with increasing angle of attack, which is a stabilizing effect.

Lateral-Directional Stability

Figure 18 indicates the effects of various model components on the lateral-directional aerodynamic characteristics. Since only a complete configuration B_9WH_3V was tested at $\beta = 0^{\circ}$ and $\beta = 5^{\circ}$, lateral-directional parameters for only this configuration are presented in figure 19. The data in figure 19 indicate that this complete configuration had positive effective dihedral $\left(-C_{l_\beta}\right)$ up to an angle of attack of about 16°. The static directional stability parameter C_{n_β} was positive at low angles but decreased with increasing angle of attack and became approximately zero at an angle of attack of approximately 10° for $R/ft = 1.7 \times 10^6$ $(R/m = 5.6 \times 10^6)$.

CONCLUSIONS

An investigation was conducted in the Langley low-turbulence pressure tunnel on a model of the second stage (orbiter) of a two-stage space shuttle concept proposed by the

NASA Manned Spacecraft Center. The tests were conducted at angles of attack from about -7° to 76° to examine the subsonic pitch-down maneuver from high to low angles as well as to obtain some basic stability and control data at low angles of attack. The two-stage launch configuration was simulated for testing when the basic orbiter model was assumed to represent the first stage and a scaled second stage was placed in a "piggyback" fashion in the approximate location as conceptually proposed. The tests were conducted at a Mach number of approximately 0.25 at Reynolds numbers per foot from about 1.7×10^{6} to 12.3×10^{6} (per meter from about 5.6×10^{6} to 40.4×10^{6}). Results of the investigation indicate the following conclusions:

1. The configuration is Reynolds number sensitive; for example, with increasing Reynolds number, the maximum untrimmed lift-drag ratio increased from 7.2 to 8.6 and the longitudinal stability decreased at low angles of attack.

2. The original proposed configuration was longitudinally unstable and just increasing horizontal-tail size to 1.70 of the original tail size was insufficient; positive stability was obtained when the leading-edge sweep of the horizontal tail was reduced from 70° to 41° with a simultaneous change in the planform shape from delta to clipped delta and, consequently, an area increase to 2.20 times the size of the original tail.

3. Constant longitudinal control effectiveness was maintained for elevator deflections up to $\pm 20^{\circ}$ at low angles of attack. The elevator was completely ineffective, however, at the highest test angles of attack.

4. Addition of the upper stage to form a complete launch configuration shifted the center of pressure from about 43 percent to 56 percent of the basic body length forward of the base of the fuselage.

5. The complete configuration indicated positive effective dihedral at angles of attack up to about 16° and was directionally stable at angles of attack up to about 10°.

Langley Research Center,
National Aeronautics and Space Administration,
Langley Station, Hampton, Va., January 23, 1970.

REFERENCES

1. Rainey, Robert W.: Summary of an Advanced Manned Lifting Entry Vehicle Study. NASA TM X-1159, 1965.

2. A Study to Determine the Flight Characteristics and Handling Qualities of Variable Geometry Spacecraft. Volume I – High L/D Concept With Single Pivot Two-Position Wing. NASA CR-1545, 1970.

3. Braslow, Albert L.; and Knox, Eugene C.: Simplified Method for Determination of Critical Height of Distributed Roughness Particles for Boundary-Layer Transition at Mach Numbers From 0 to 5. NACA TN 4363, 1958.

TABLE I.- GEOMETRIC CHARACTERISTICS OF MODEL

Wing W:	
Aspect ratio	7.0
Span, in. (cm)	18.00 (45.72)
Area, total, ft^2 (m^2)	0.320 (0.030)
Area, exposed, ft^2 (m^2)	0.274 (0.025)
Root chord at fuselage center line, in. (cm)	3.84 (9.75)
Tip chord, in. (cm)	1.28 (3.25)
Mean geometric chord, in. (cm)	2.78 (7.06)
Airfoil section:	
Root	NACA 0014-64
Tip	NACA 0010-64
Leading-edge sweep angle, deg	14
Dihedral angle, deg	8.25
Taper ratio	0.333
Fuselage B_9:	
Length, in. (cm)	25.70 (65.28)
Ramp angle, deg	9
Balance-chamber and base area, ft^2 (m^2)	0.0494 (0.0046)
Planform area, ft^2 (m^2)	0.604 (0.056)
Fuselage B_{20}:	
Length, in. (cm)	25.12 (63.80)
Ramp angle, deg	20
Balance-chamber and base area, ft^2 (m^2)	0.0494 (0.0046)
Planform area, ft^2 (m^2)	0.580 (0.054)
Horizontal tail H_1:	
Area, exposed (including area behind fuselage), ft^2 (m^2)	0.0754 (0.0070)
Airfoil section	NACA 0012-64
Leading-edge sweep angle, deg	70
Horizontal tail H_2:	
Area, exposed (including area behind fuselage), ft^2 (m^2)	0.1279 (0.0119)
Airfoil section	NACA 0012-64
Leading-edge sweep angle, deg	70
Horizontal tail H_3:	
Area, exposed (including area behind fuselage), ft^2 (m^2)	0.1656 (0.0154)
Airfoil section	Slab with feathered trailing edge
Leading-edge sweep angle, deg	41
Vertical tail V:	
Area, ft^2 (m^2)	0.0684 (0.0064)
Airfoil section	NACA 0012-64

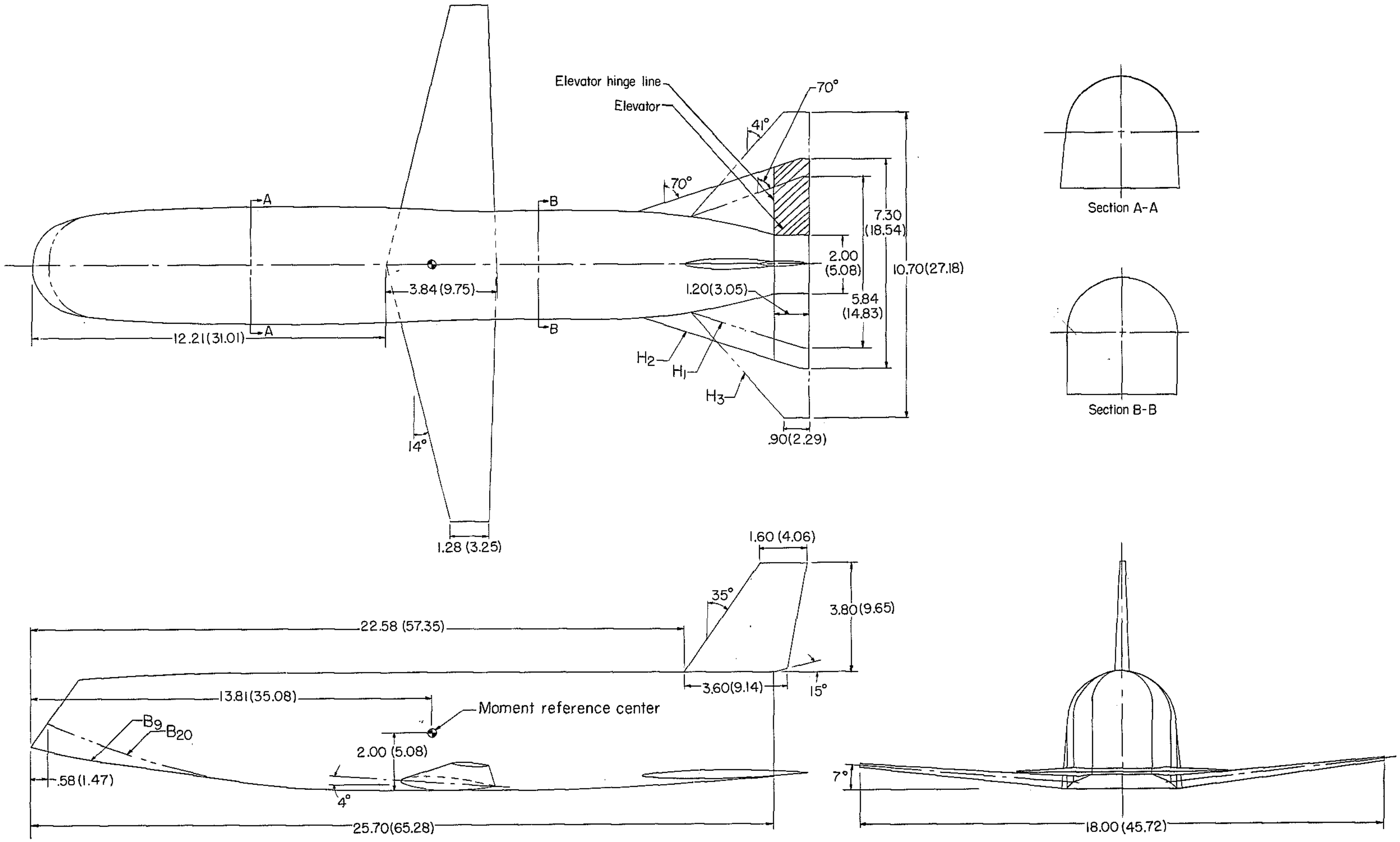

(a) Orbiter.

Figure 1.- Details of models. All linear dimensions are in inches (centimeters).

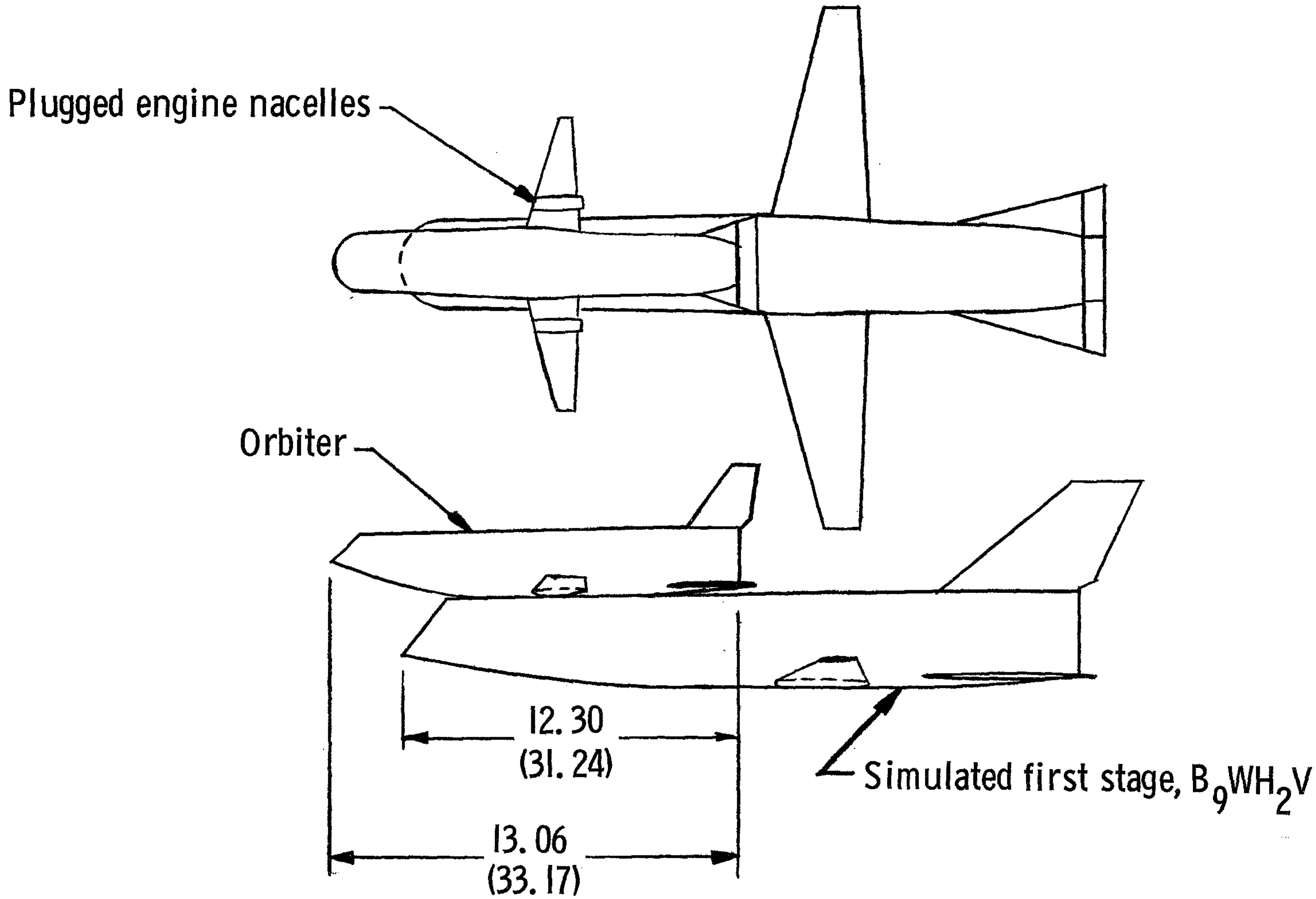

(b) Simulated launch configuration.

Figure 1.- Concluded.

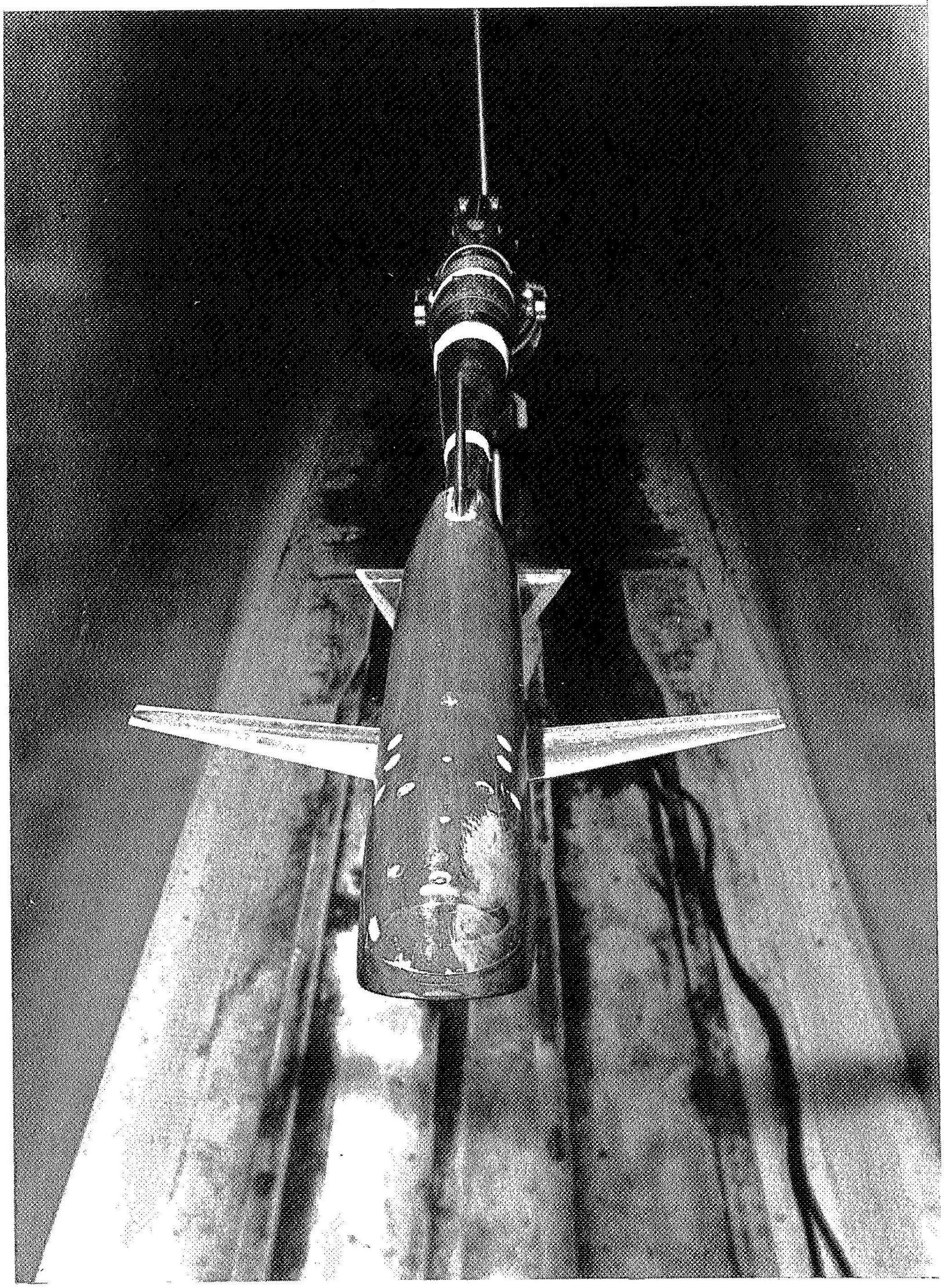

(a) Front view of $B_{20}WH_2V$. L-69-5927

Figure 2.- Photographs of model.

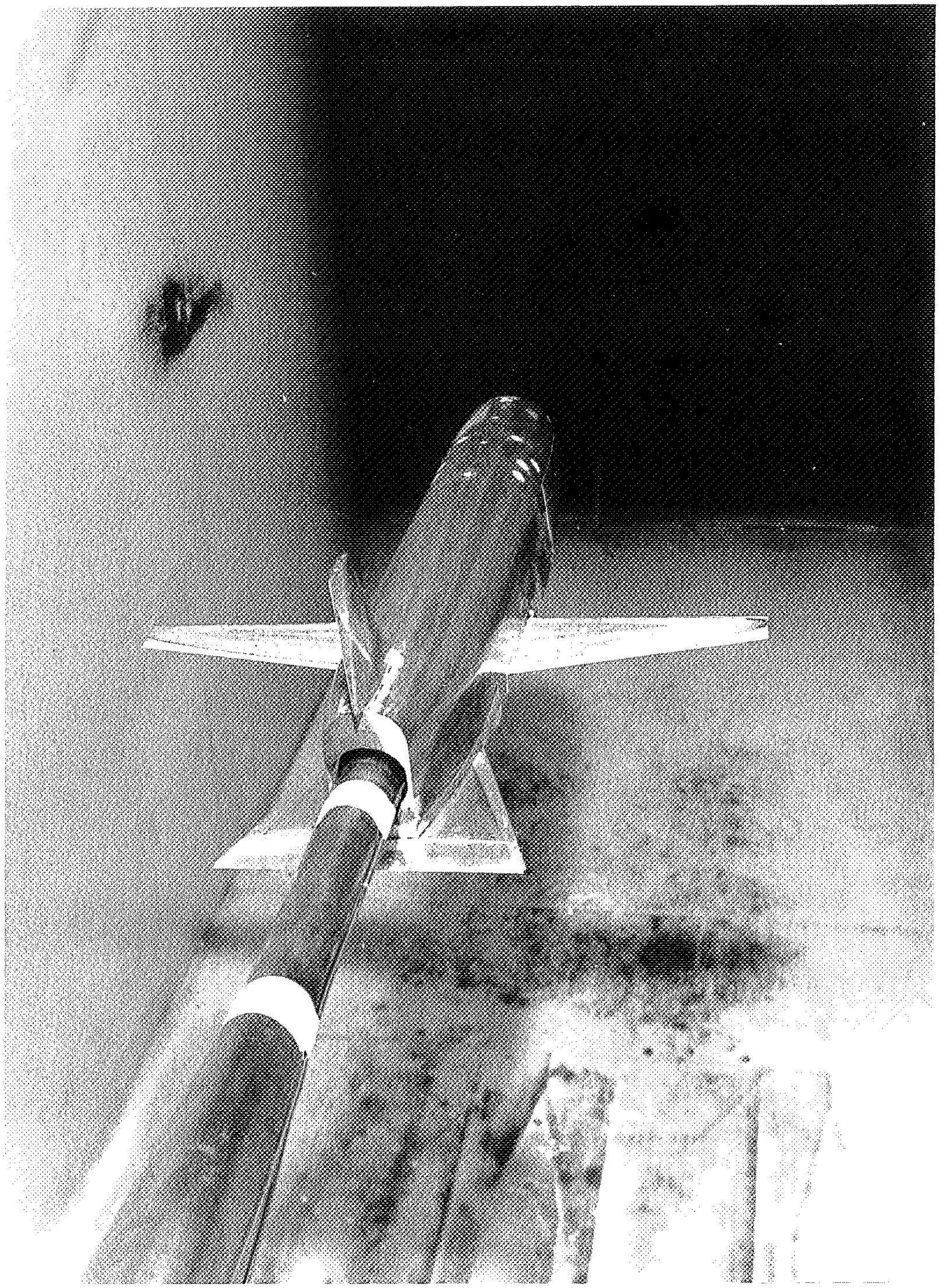

(b) Rear view of $B_{20}WH_2V$. L-69-5928

Figure 2.- Continued.

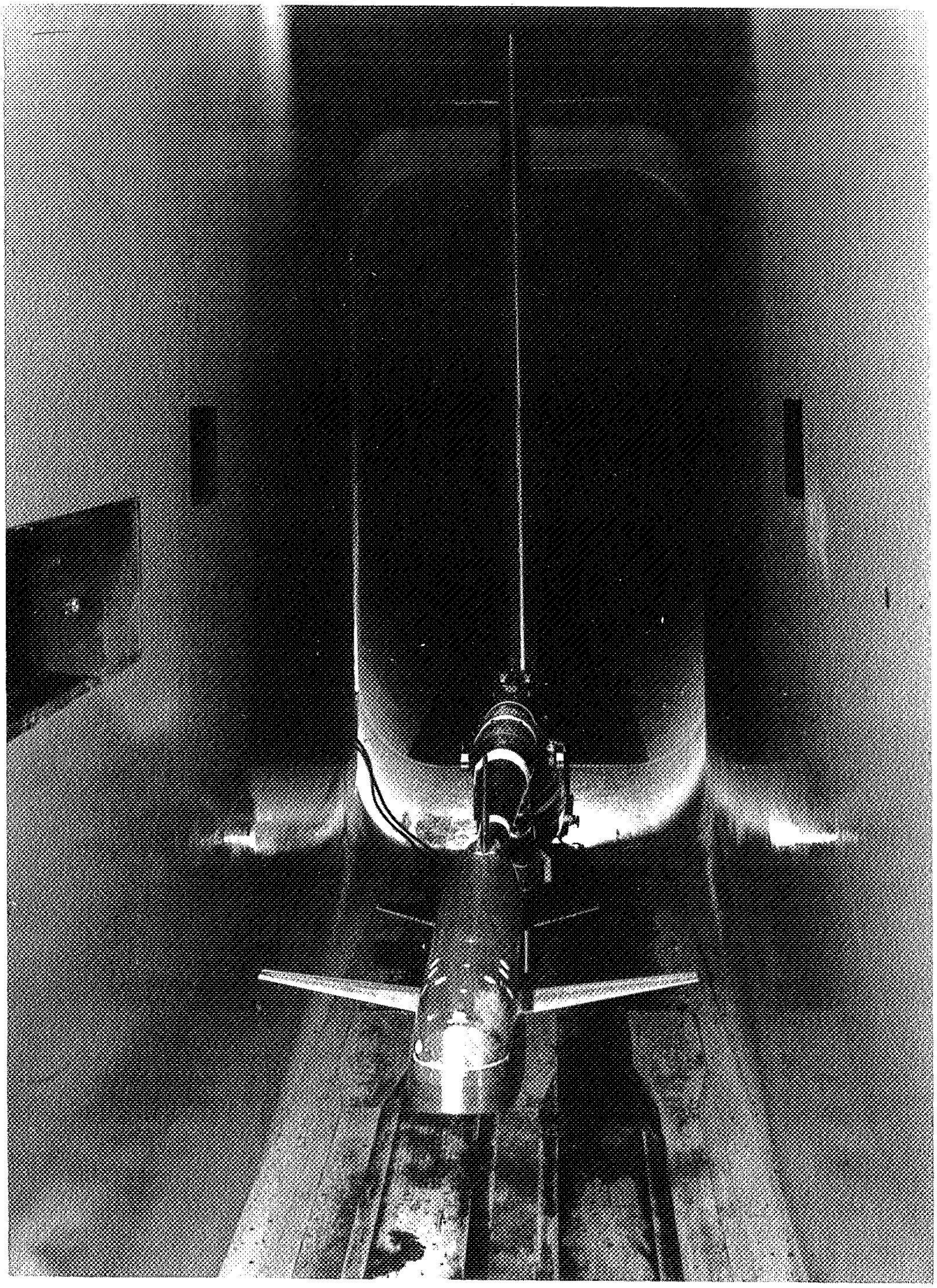

(c) Front view of B_9WH_3V. L-69-5922

Figure 2.- Continued.

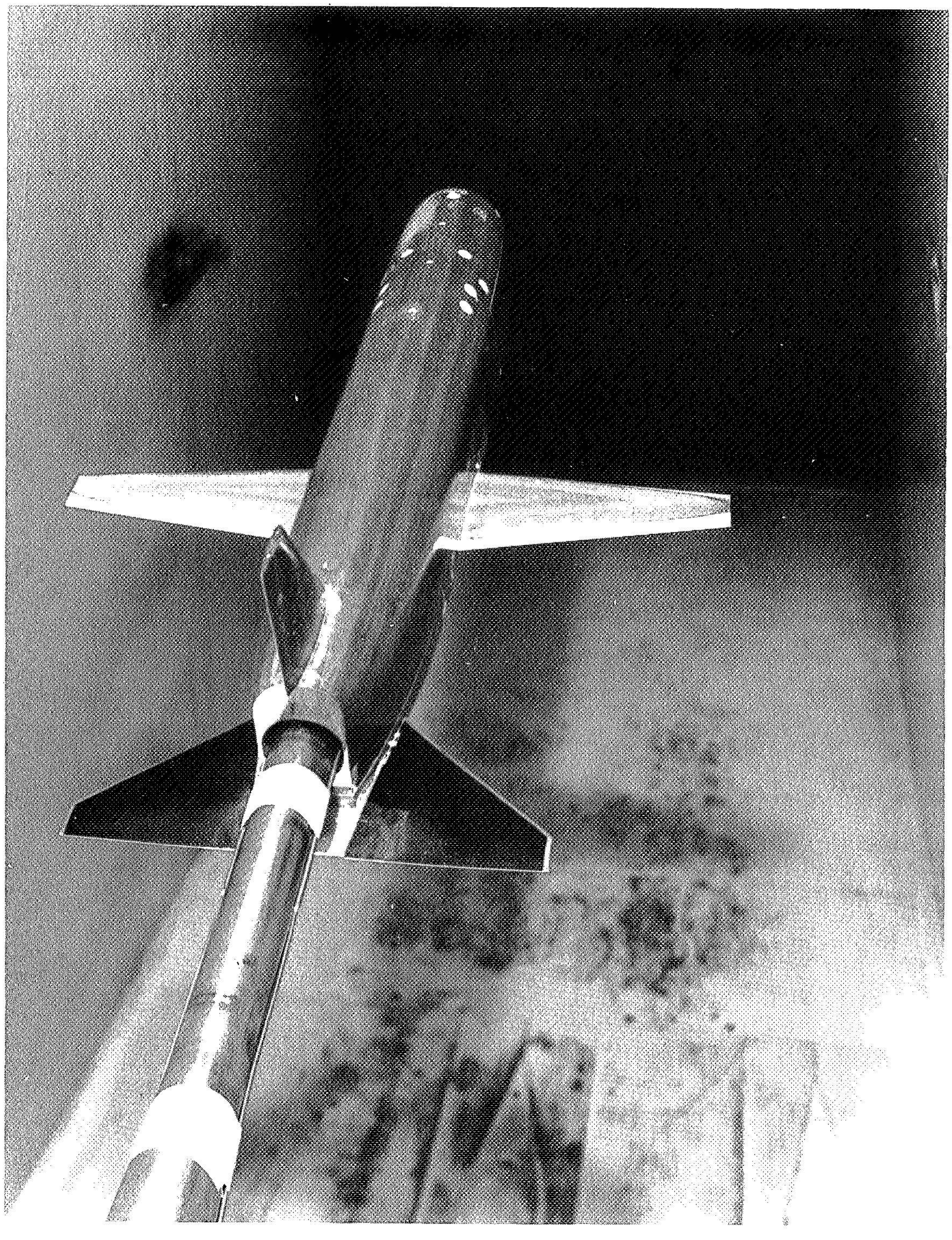

(d) Rear view of B_9WH_3V. L-69-5923

Figure 2.- Continued.

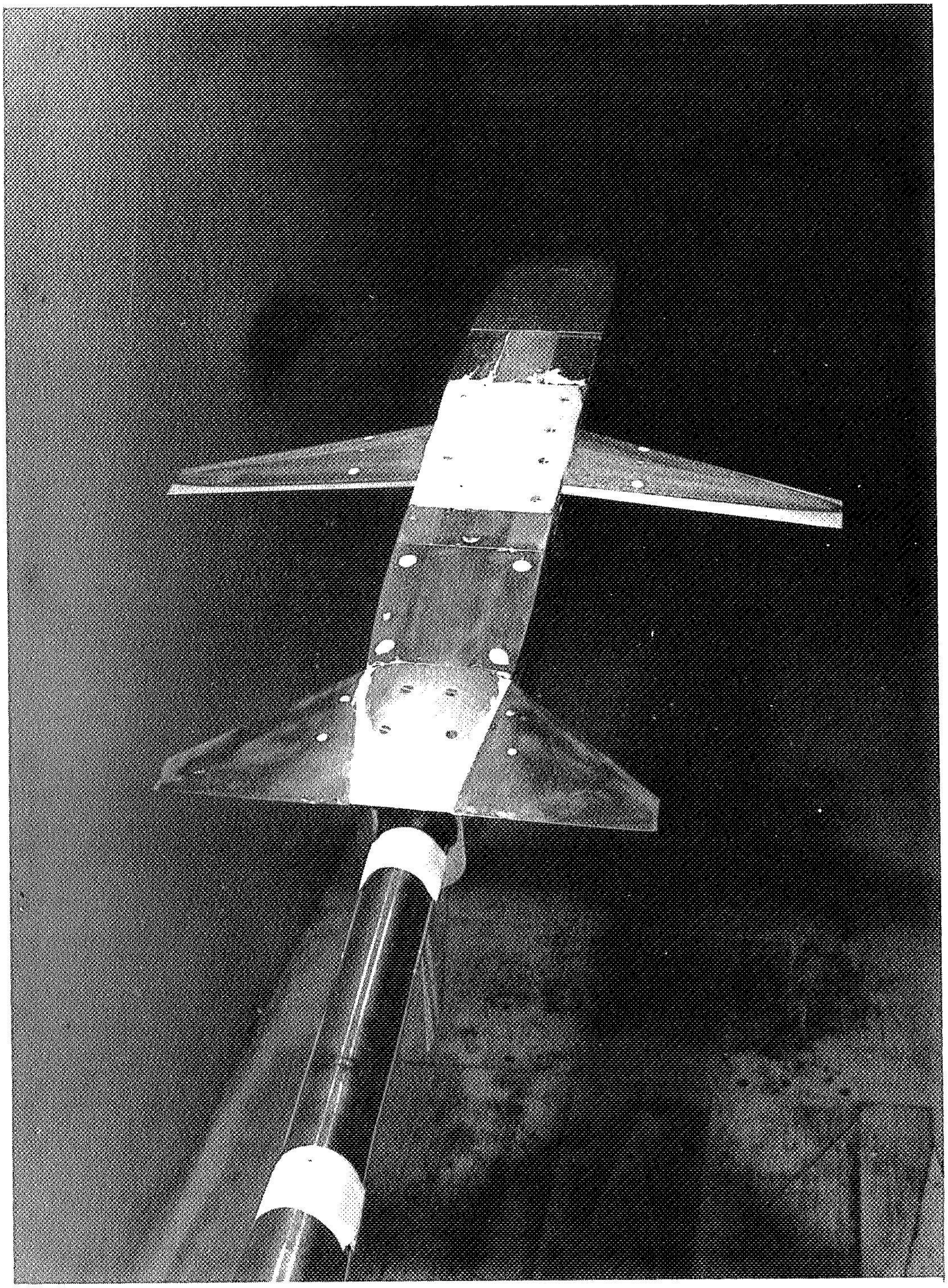

(e) Bottom view of B_9WH_3V. L-69-5925

Figure 2.- Concluded.

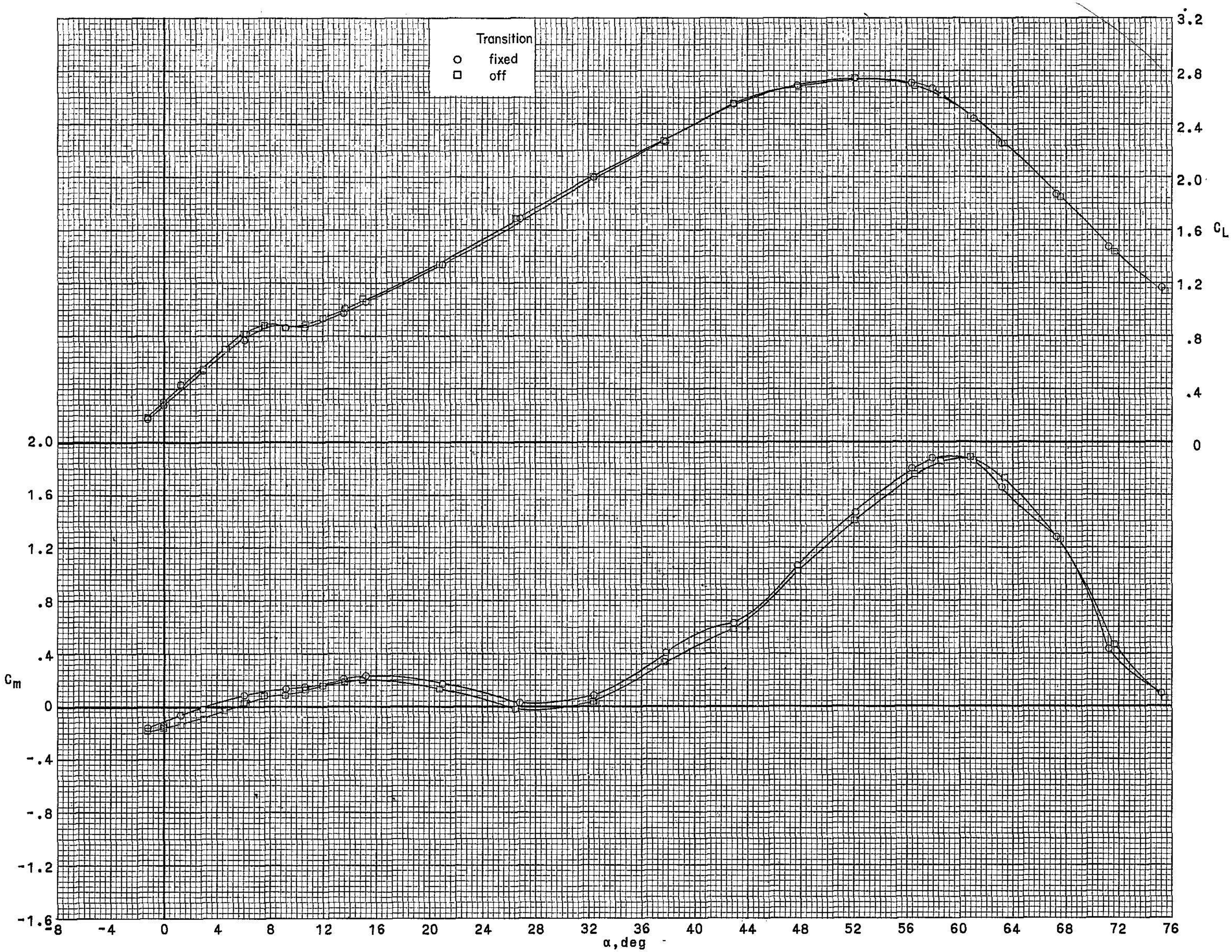

Figure 3.- Effect of transition strips on longitudinal aerodynamic characteristics of B_9WH_2V. $\delta_e = 0^o$; R/ft = 1.7×10^6 (R/m = 5.6×10^6).

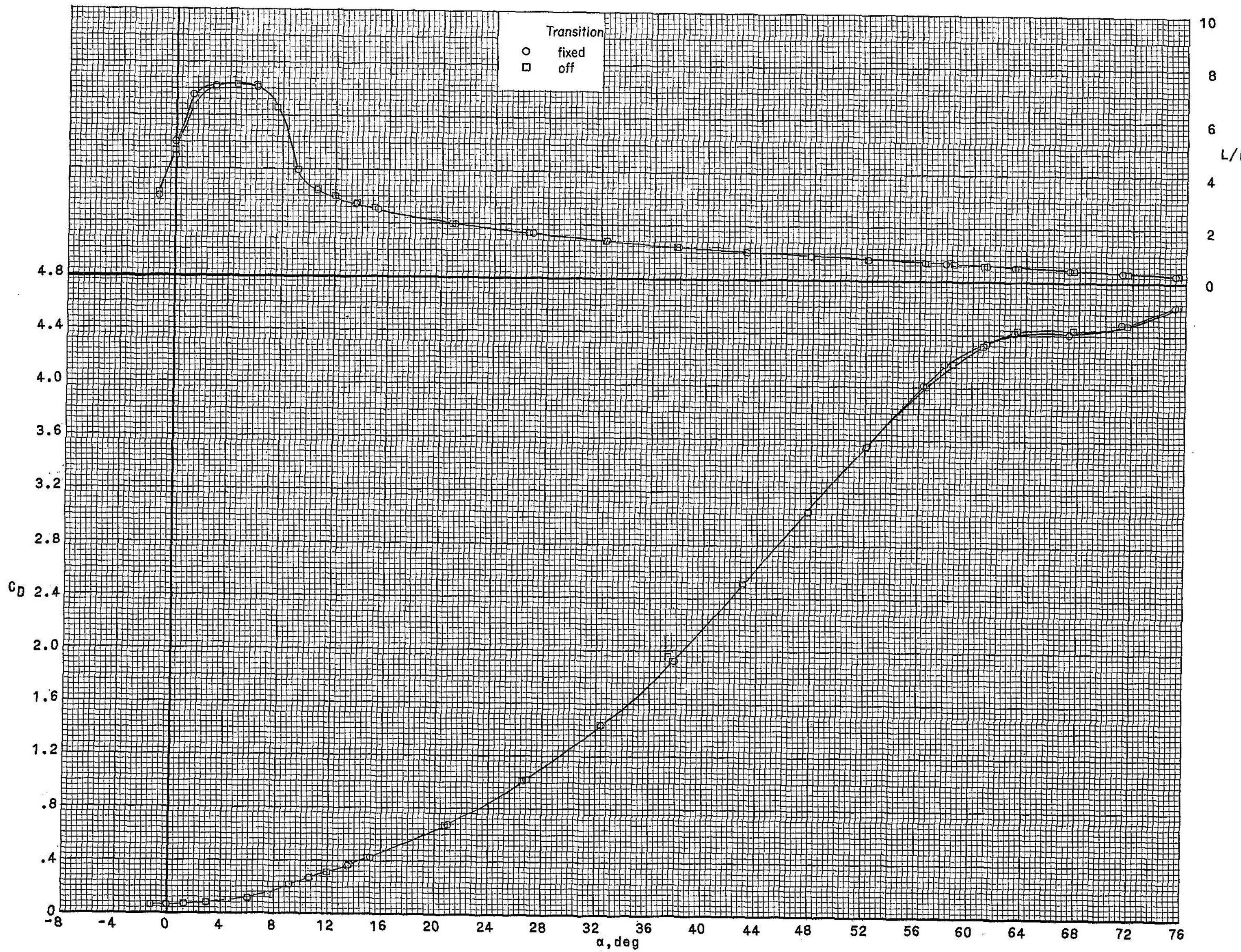

Figure 3.- Concluded.

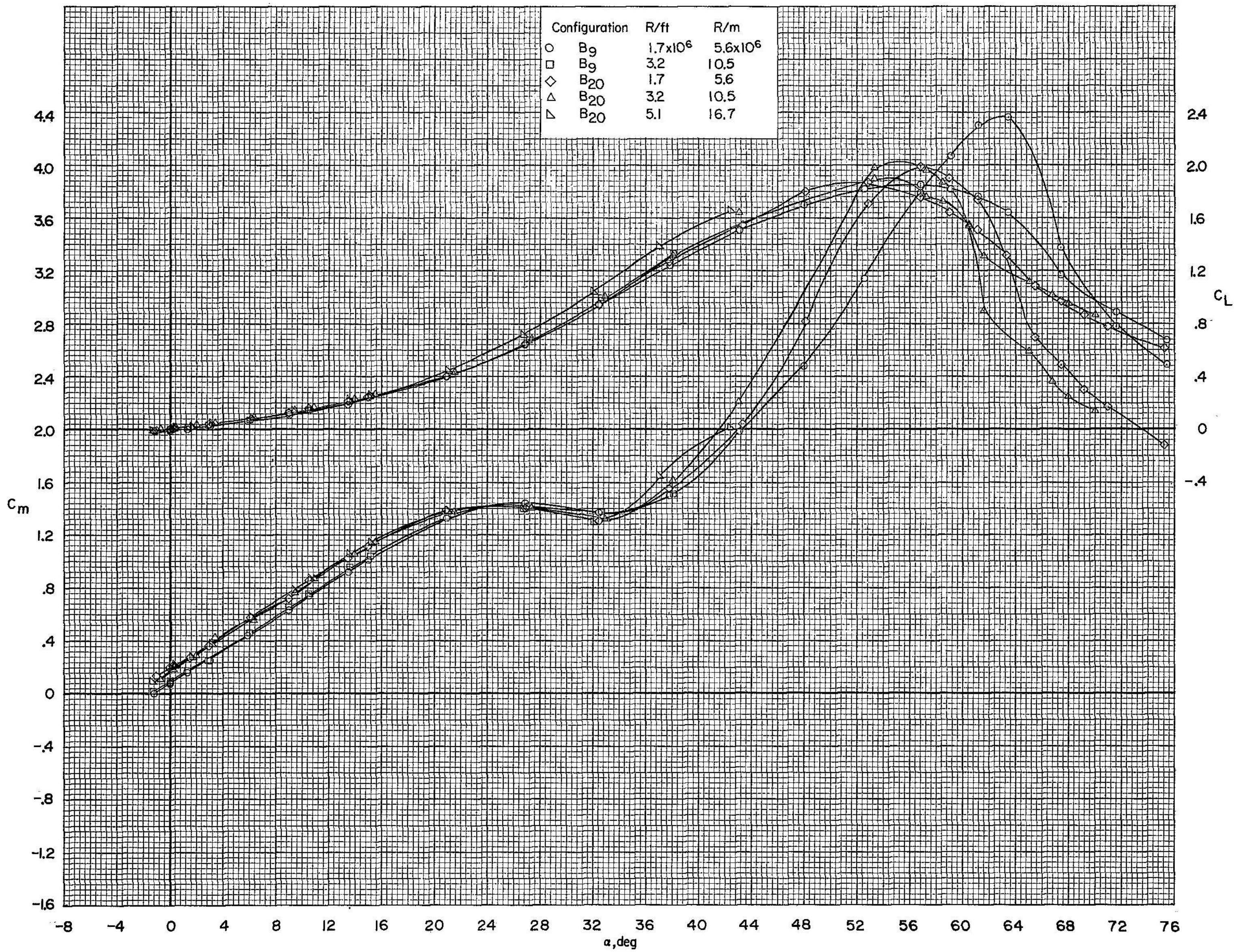

Figure 4.- Effect of nose ramp angle on longitudinal aerodynamic characteristics.

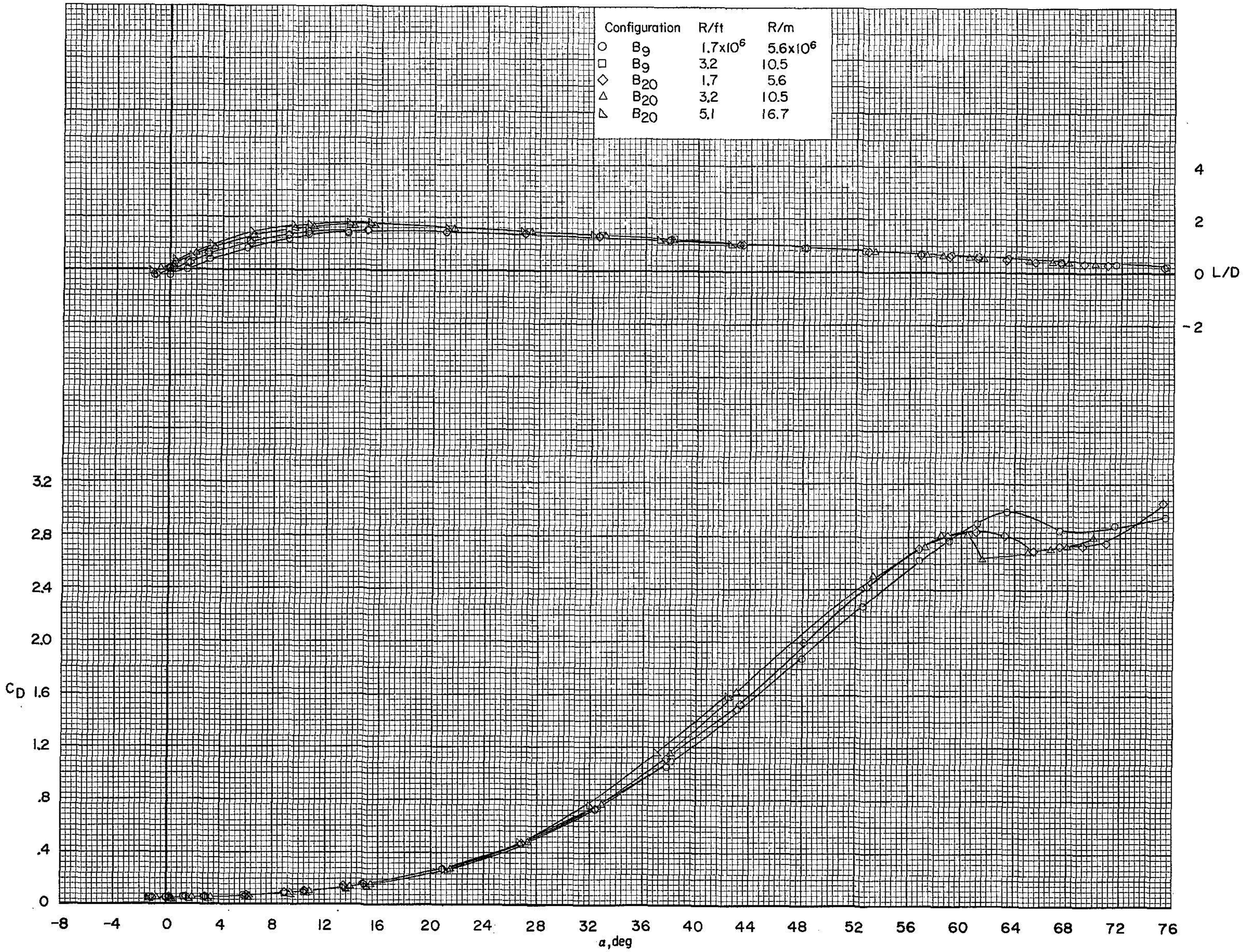

Figure 4.- Concluded.

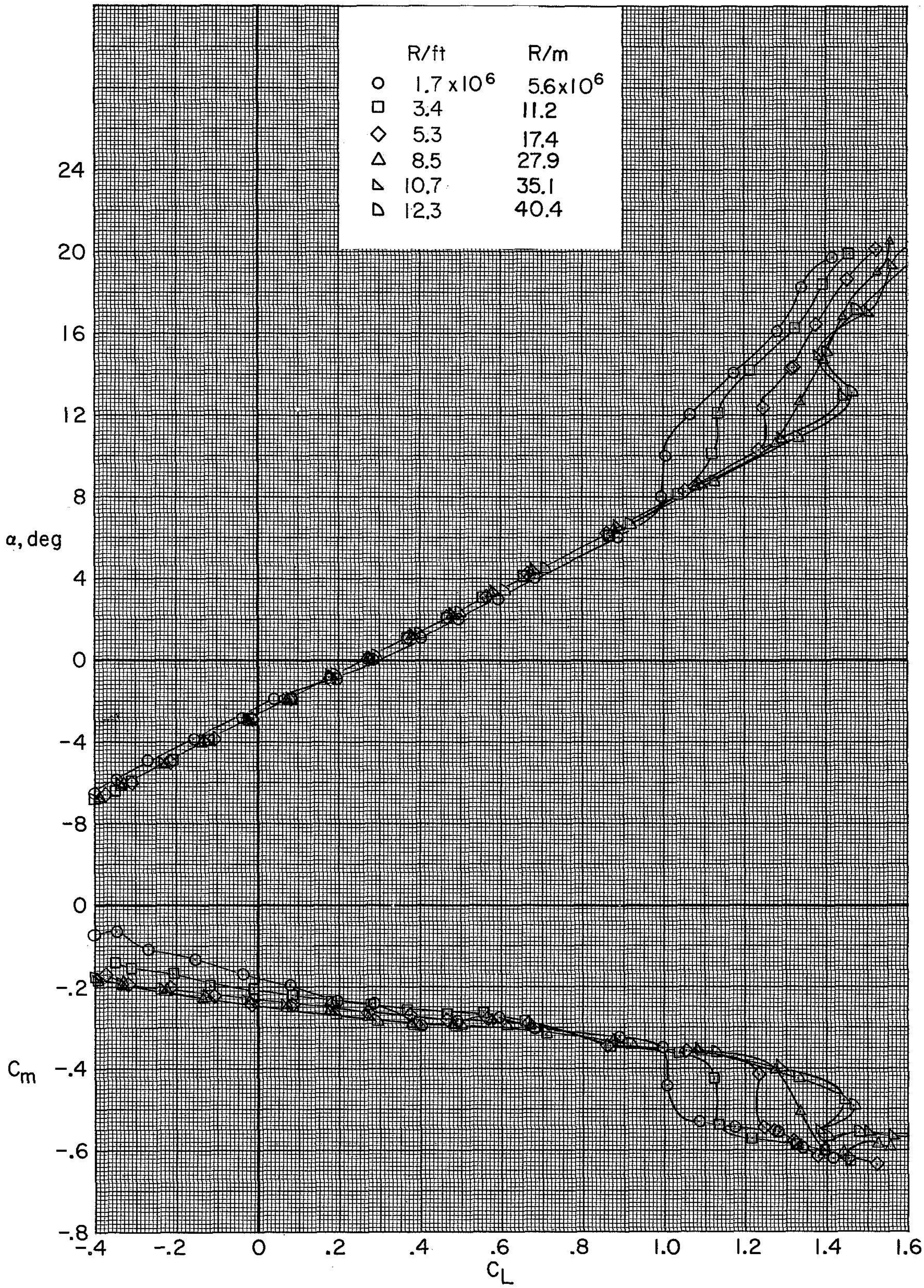

Figure 5.- Effect of Reynolds number on longitudinal aerodynamic characteristics of B_9WH_3V. $\delta_e = 0^o$.

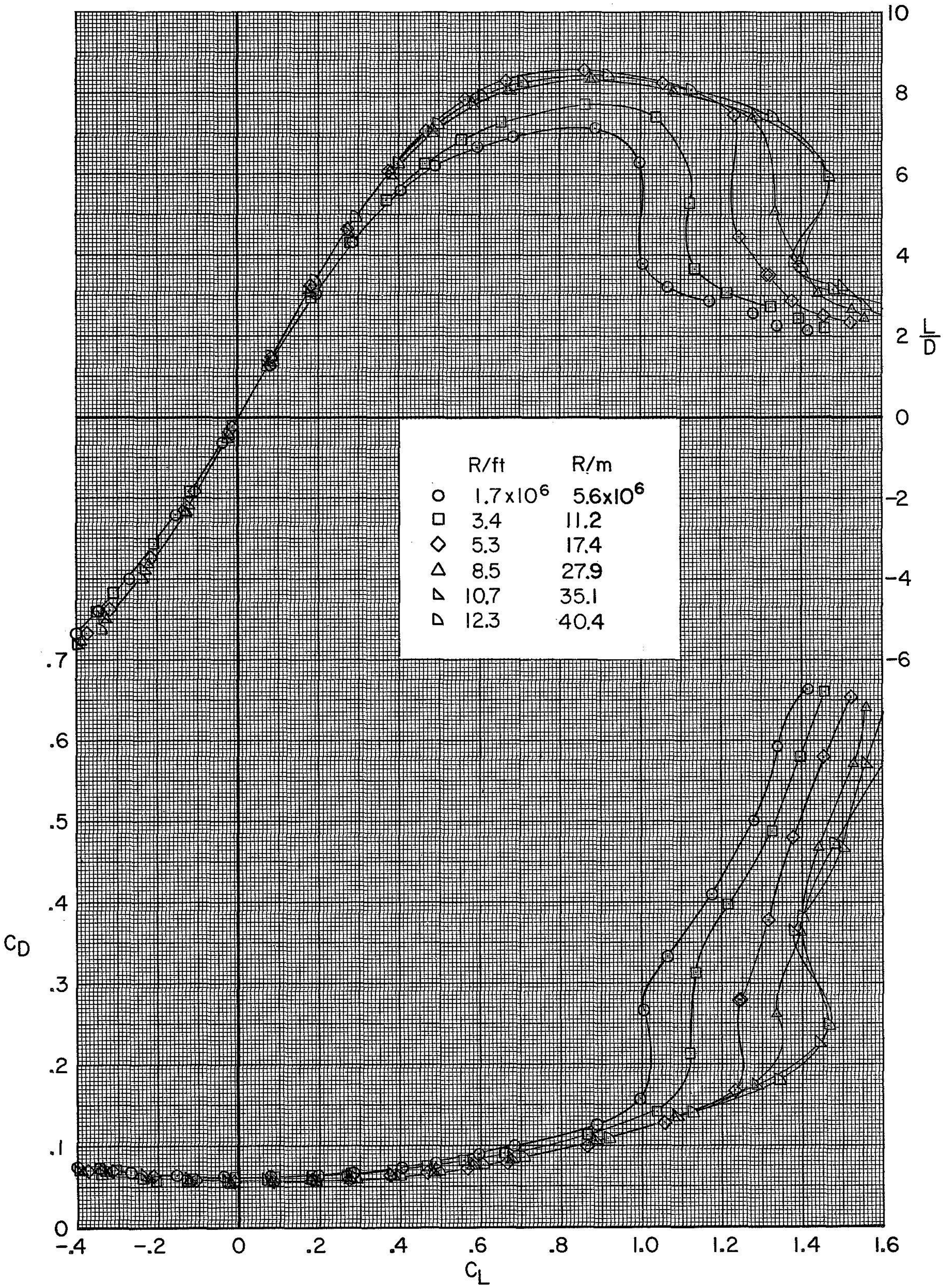

Figure 5.- Concluded.

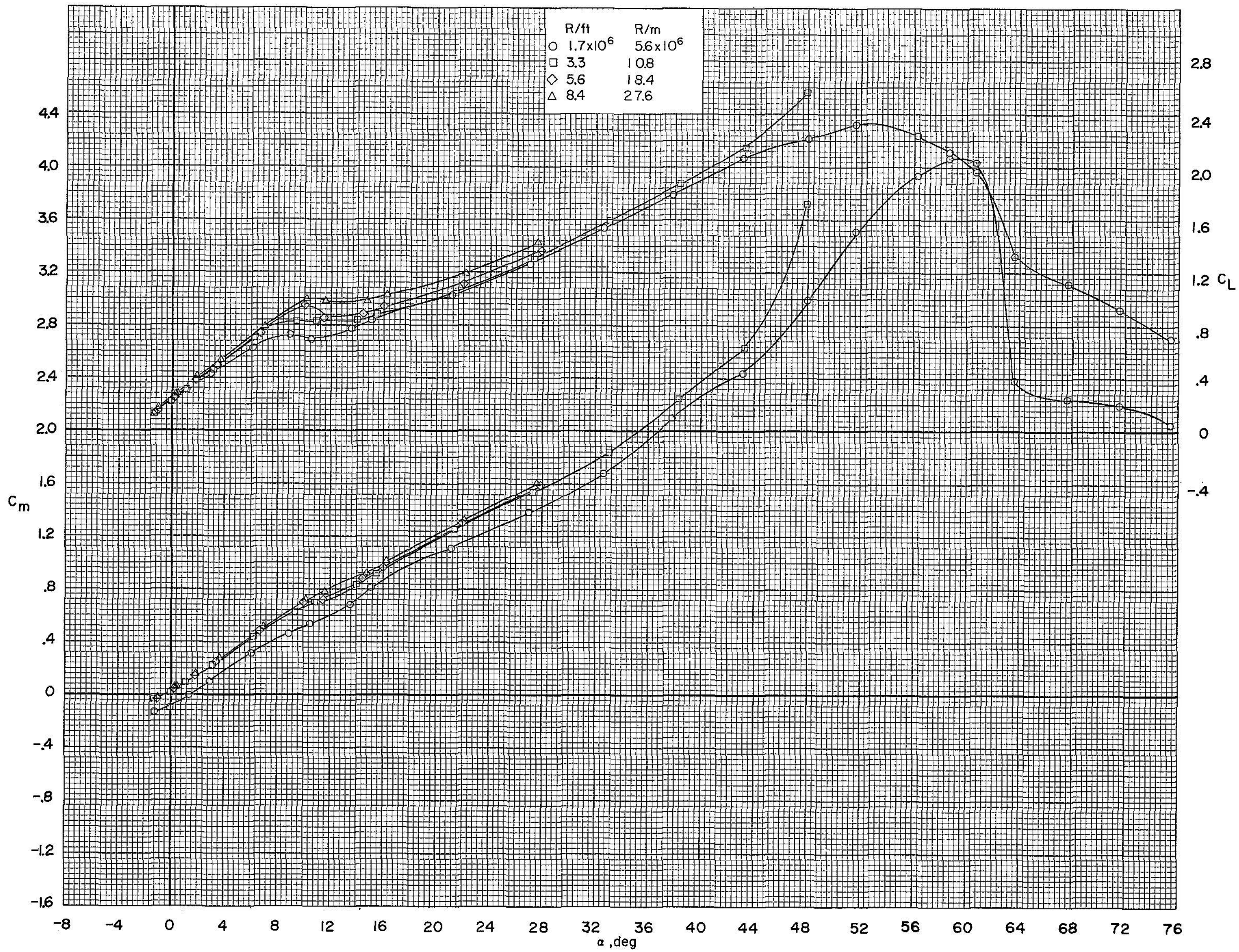

Figure 6.- Effect of Reynolds number on longitudinal aerodynamic characteristics of B_9WV. $\delta_e = 0^0$.

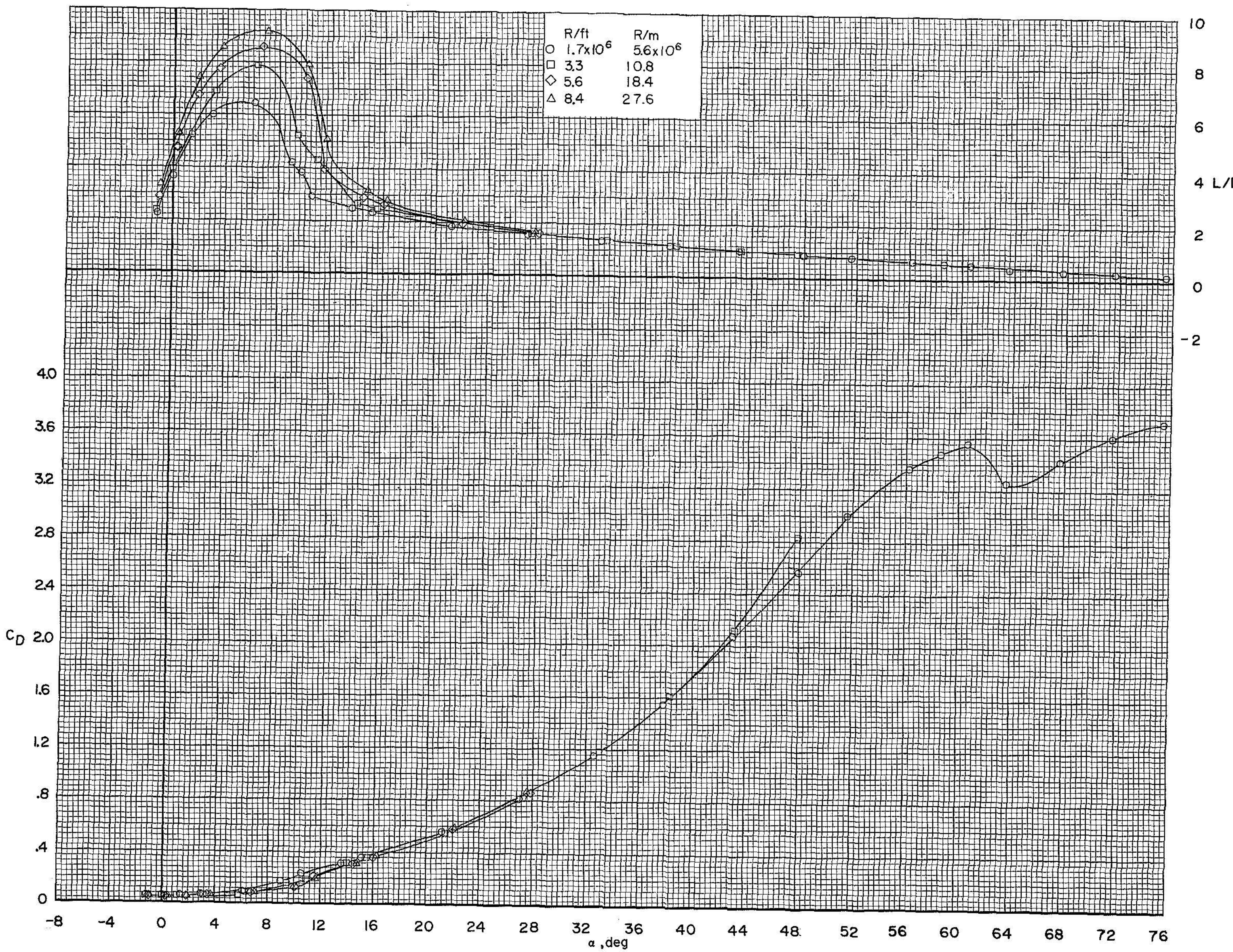

Figure 6.- Concluded.

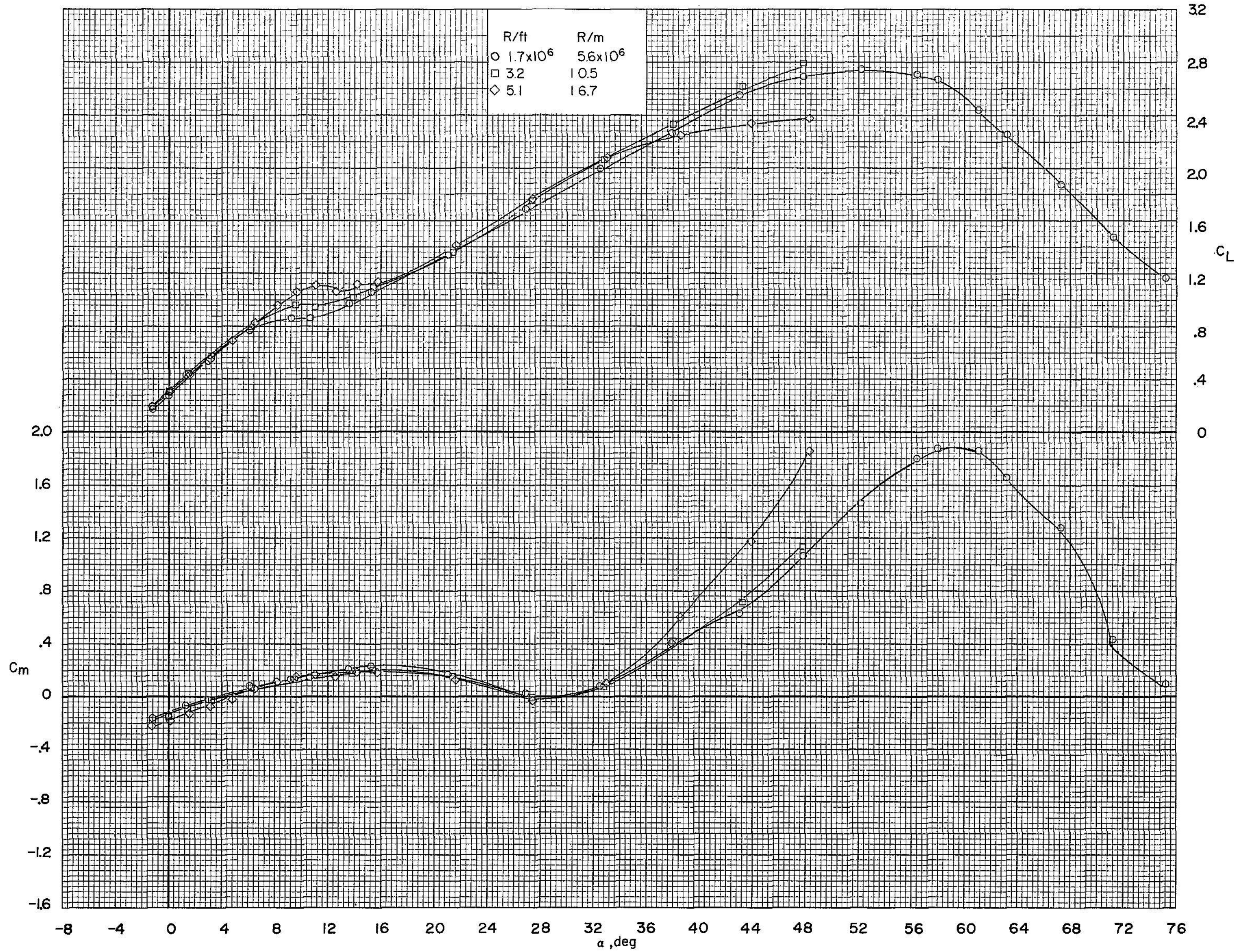

Figure 7.- Effect of Reynolds number on longitudinal aerodynamic characteristics of B_9WH_2V. $\delta_e = 0^0$.

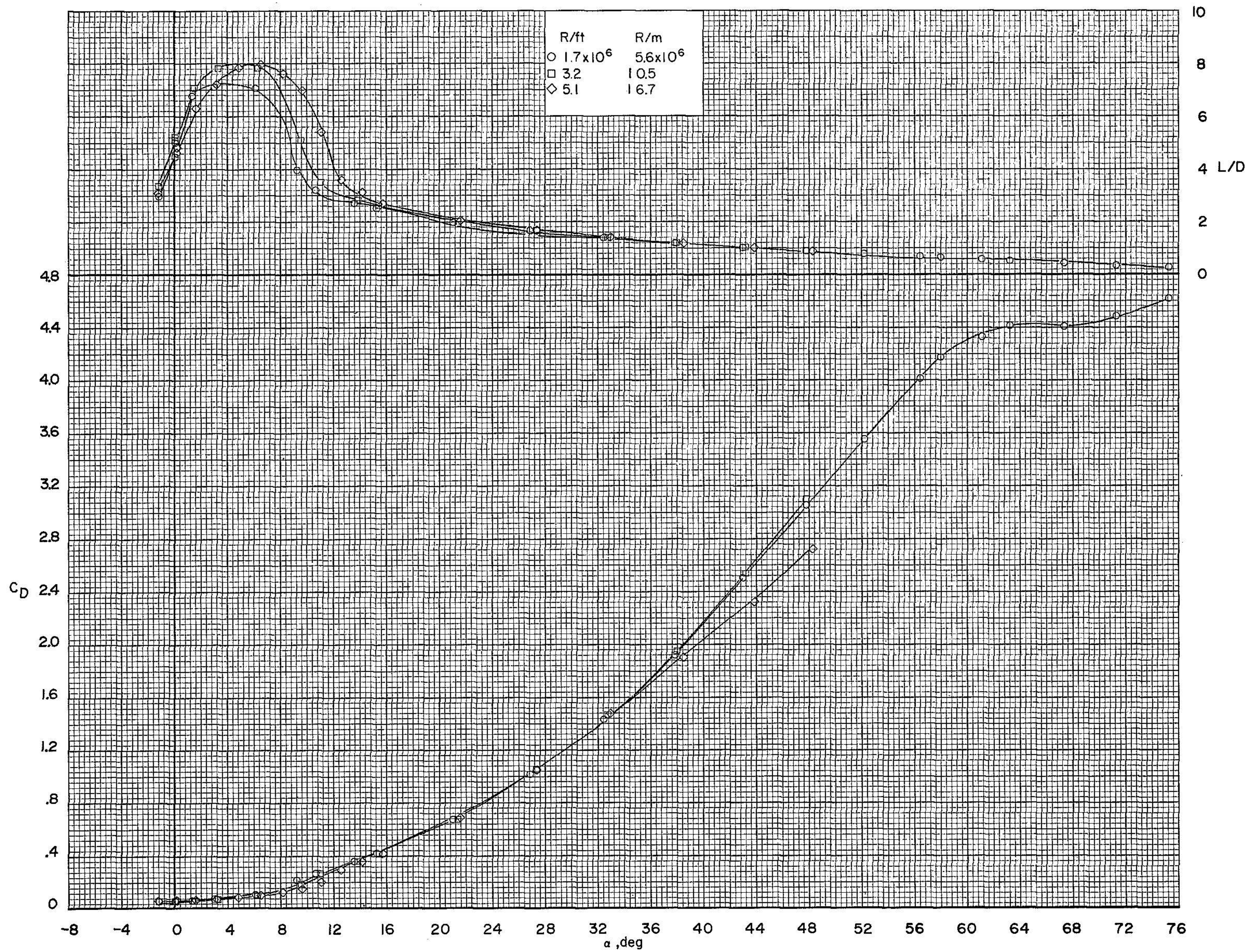

Figure 7.- Concluded.

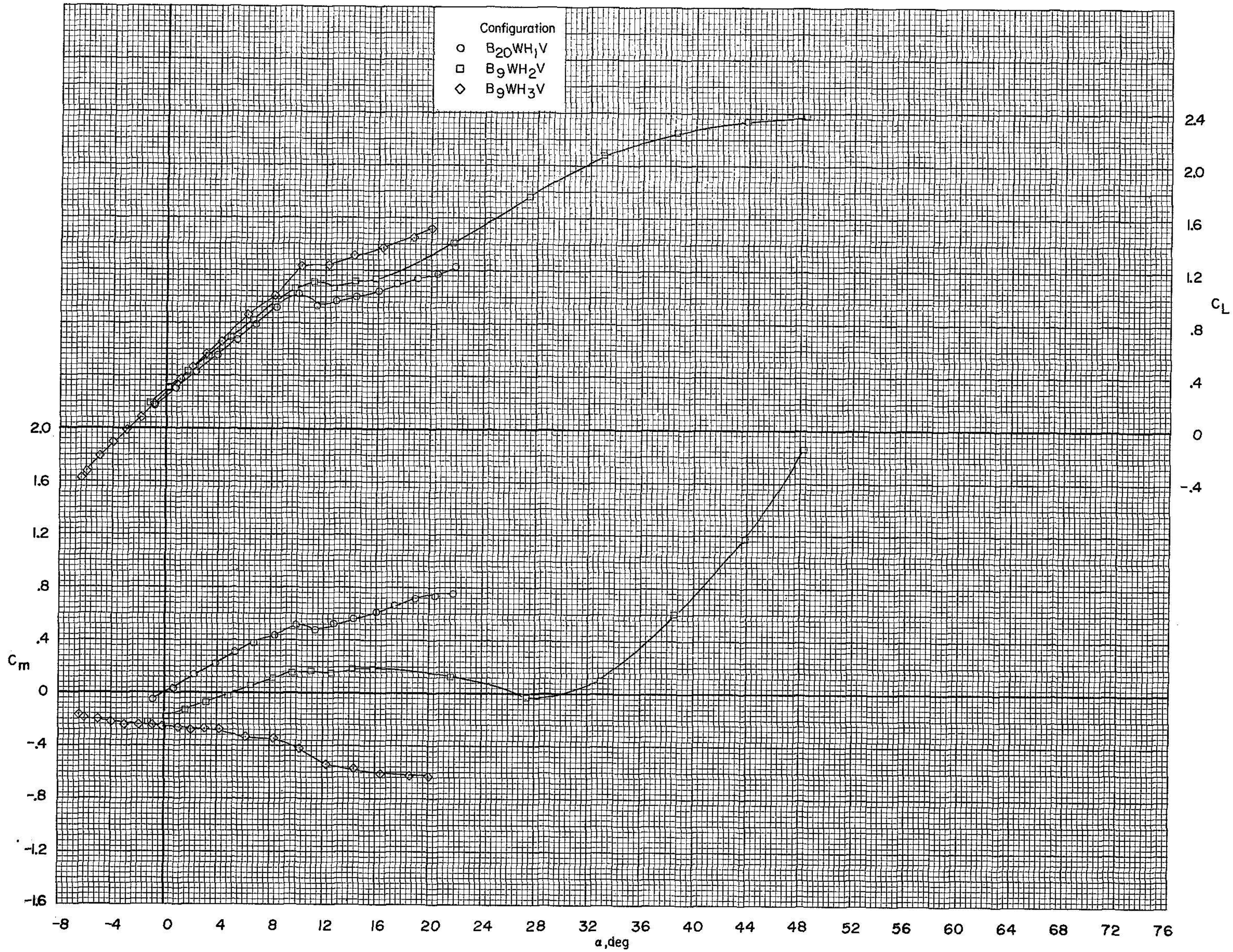

Figure 8.- Effect of horizontal-tail size on longitudinal aerodynamic characteristics. $\delta_e = 0^0$; R/ft = 5.1×10^6 (R/m = 16.7×10^6).

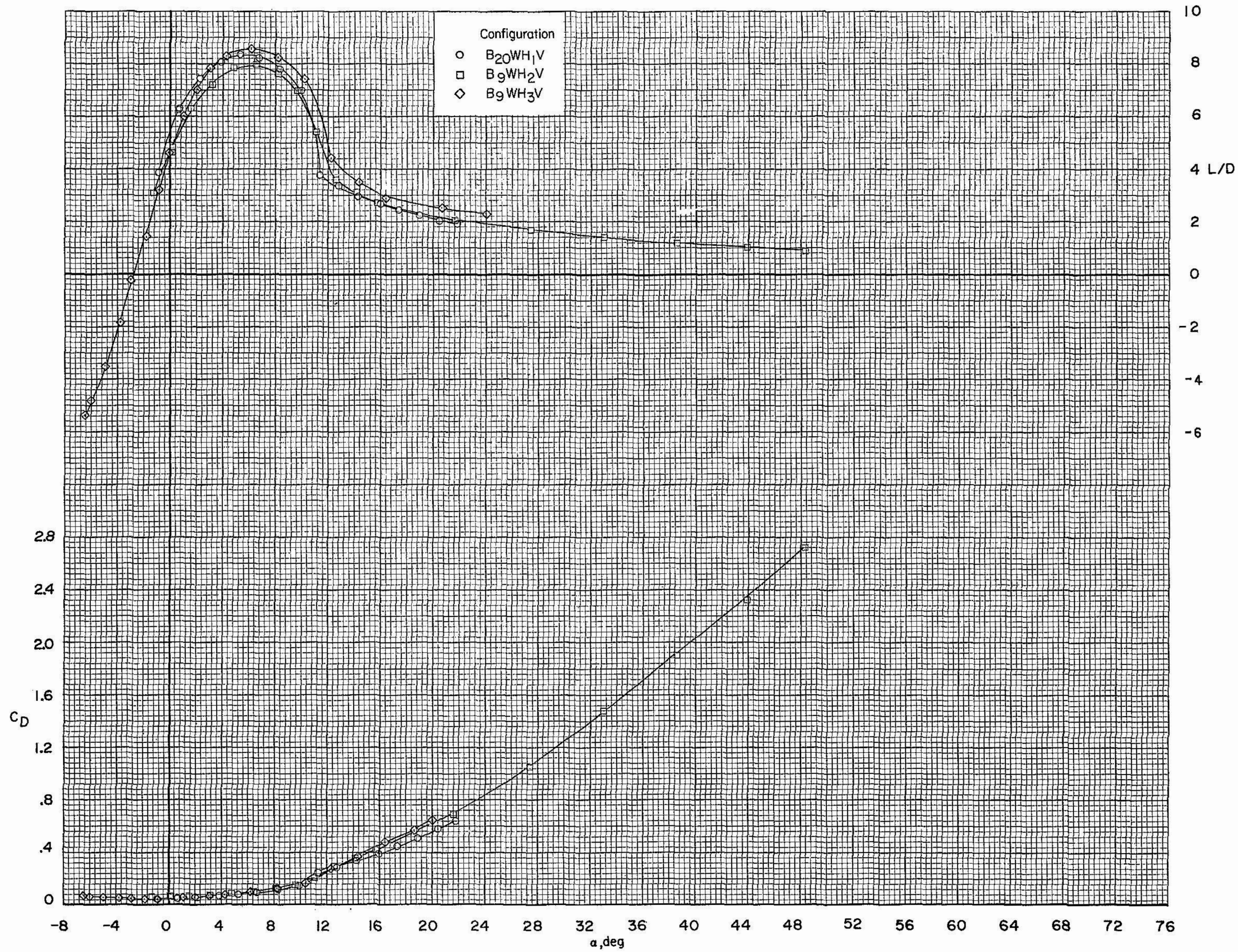

Figure 8.- Concluded.

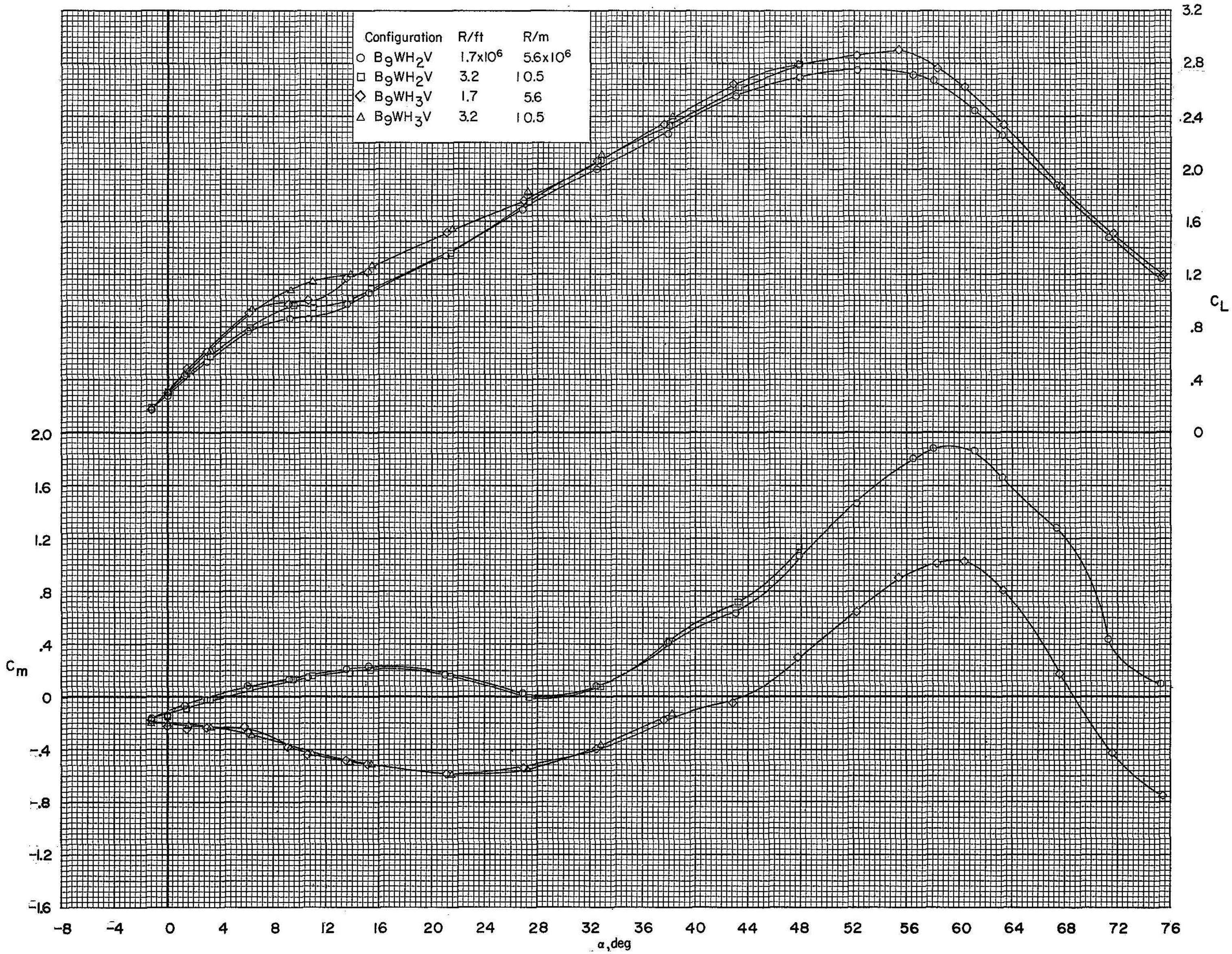

Figure 9.- Effect of horizontal-tail size on longitudinal aerodynamic characteristics. $\delta_e = 0^0$; R/ft = 1.7×10^6 and 3.2×10^6 (R/m = 5.6×10^6 and 10.5×10^6).

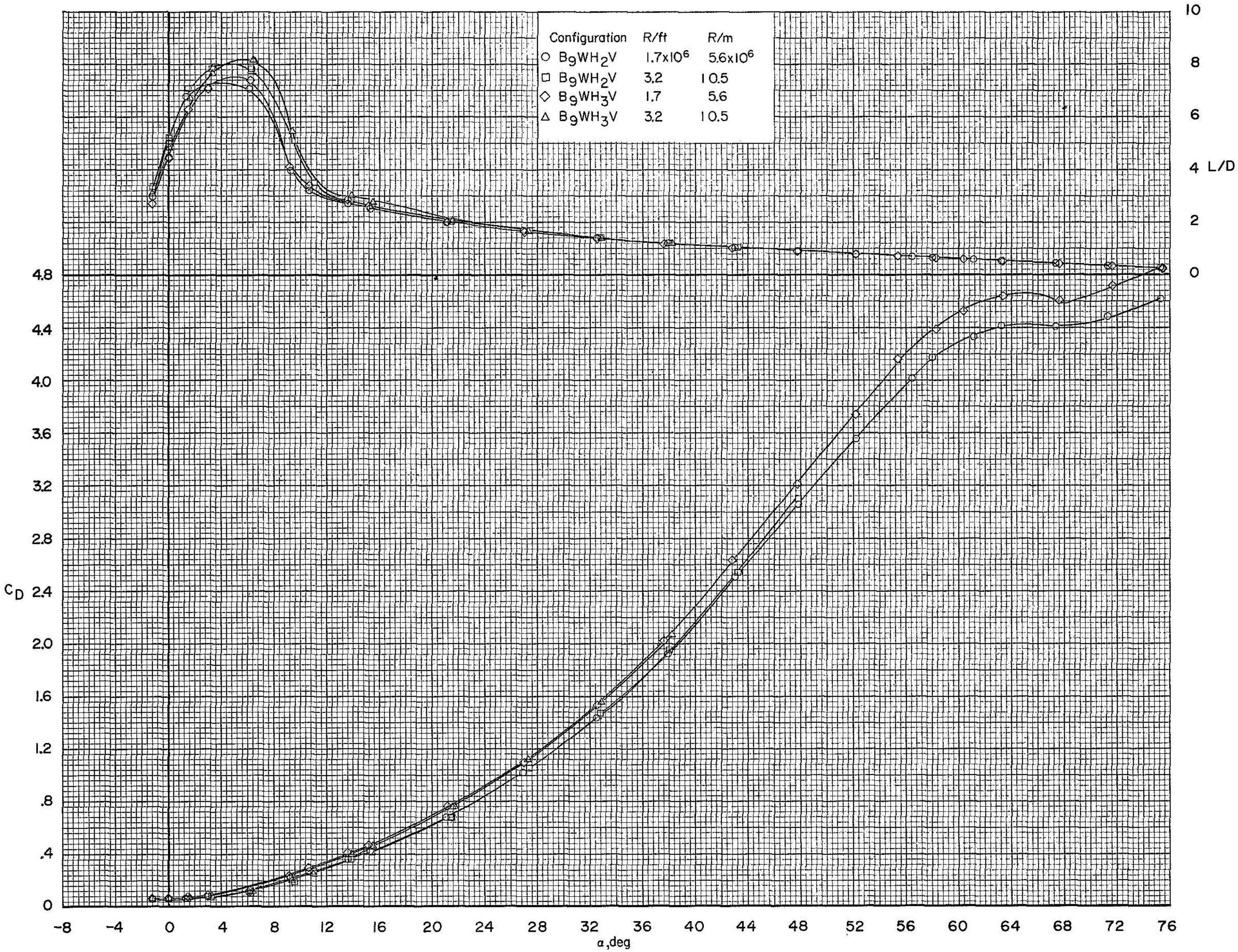

Figure 9.- Concluded.

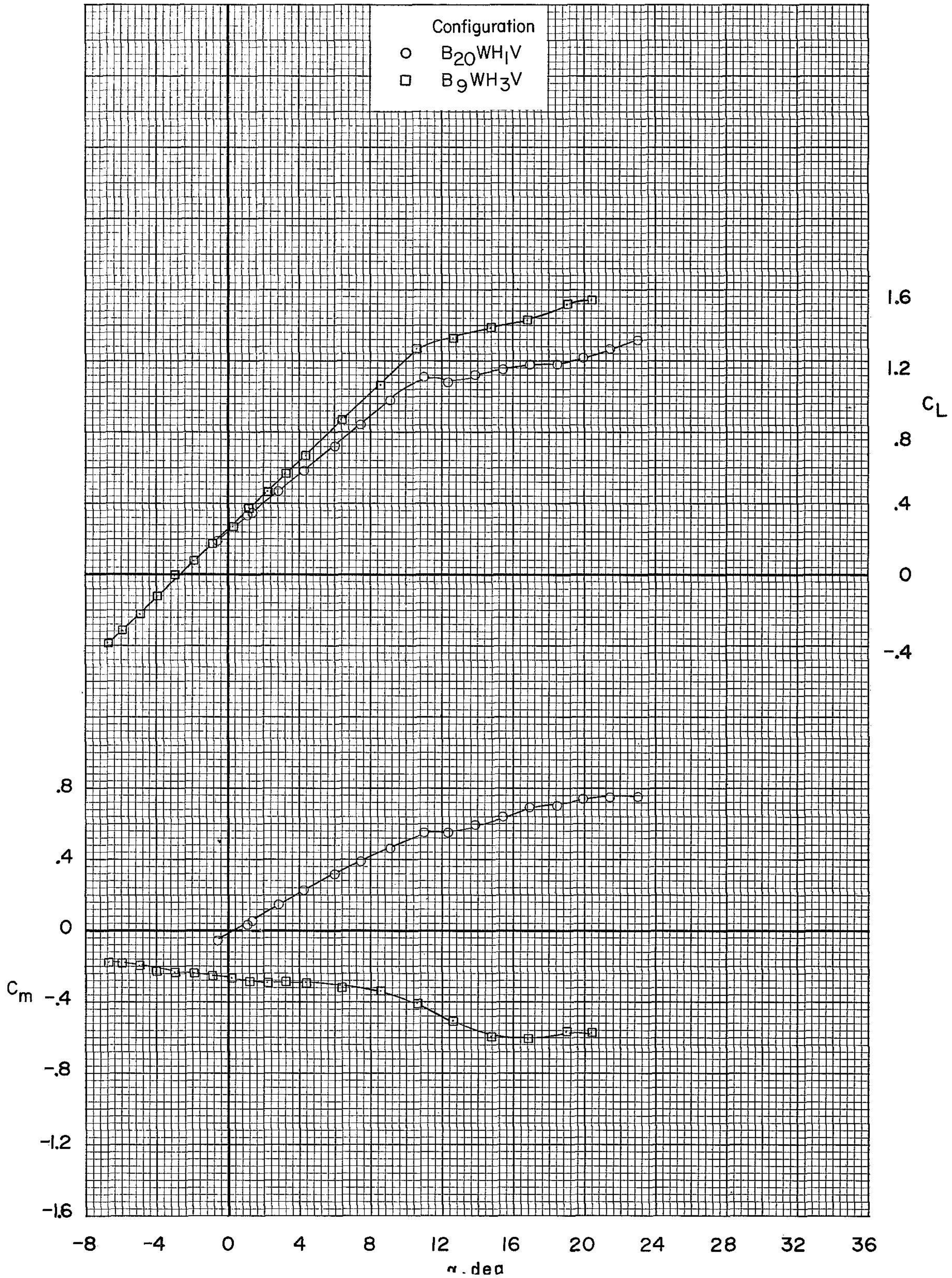

Figure 10.- Effect of horizontal-tail size on longitudinal aerodynamic characteristics. $\delta_e = 0^0$; R/ft = 8.4×10^6 (R/m = 27.6×10^6).

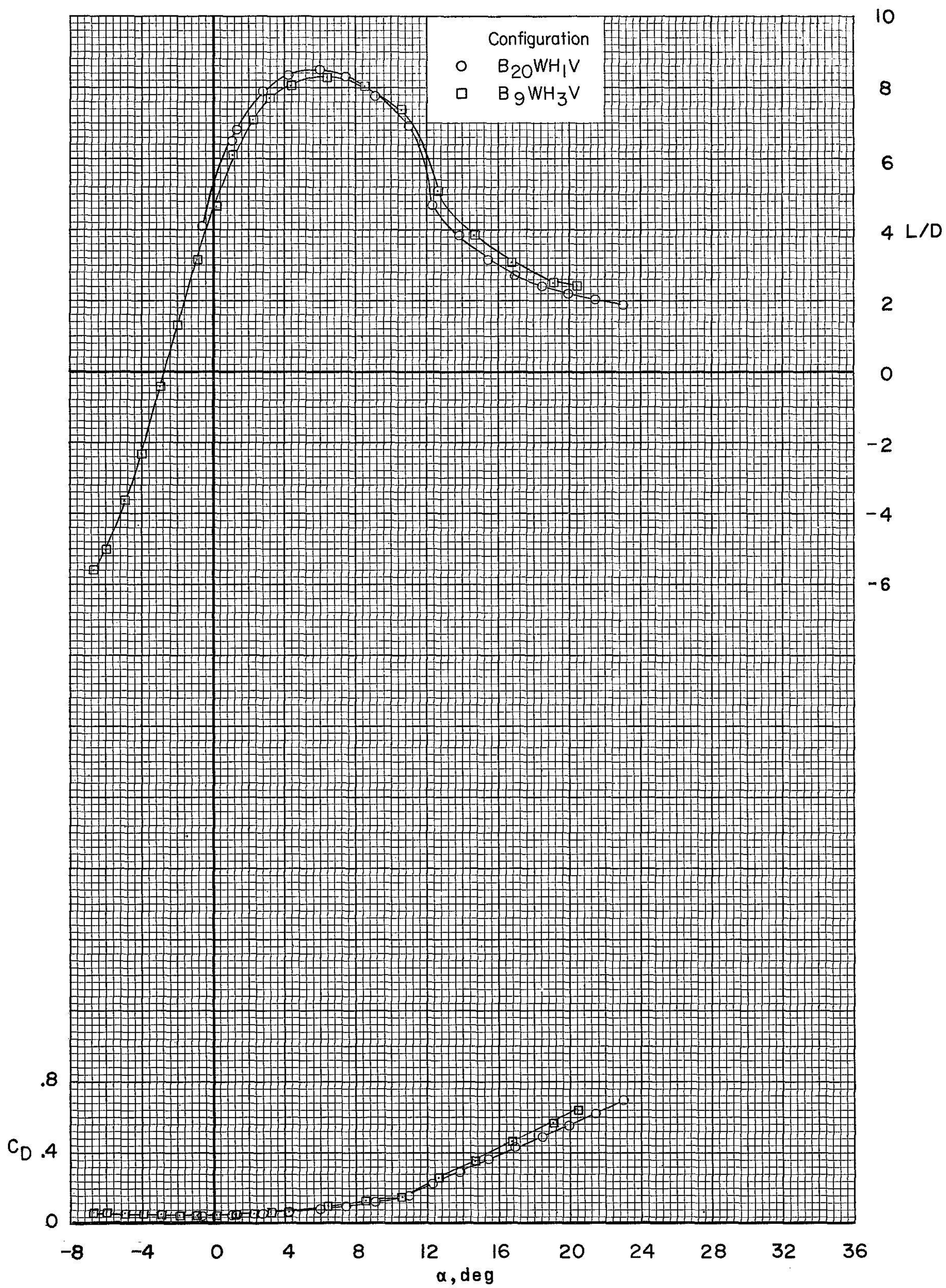

Figure 10.- Concluded.

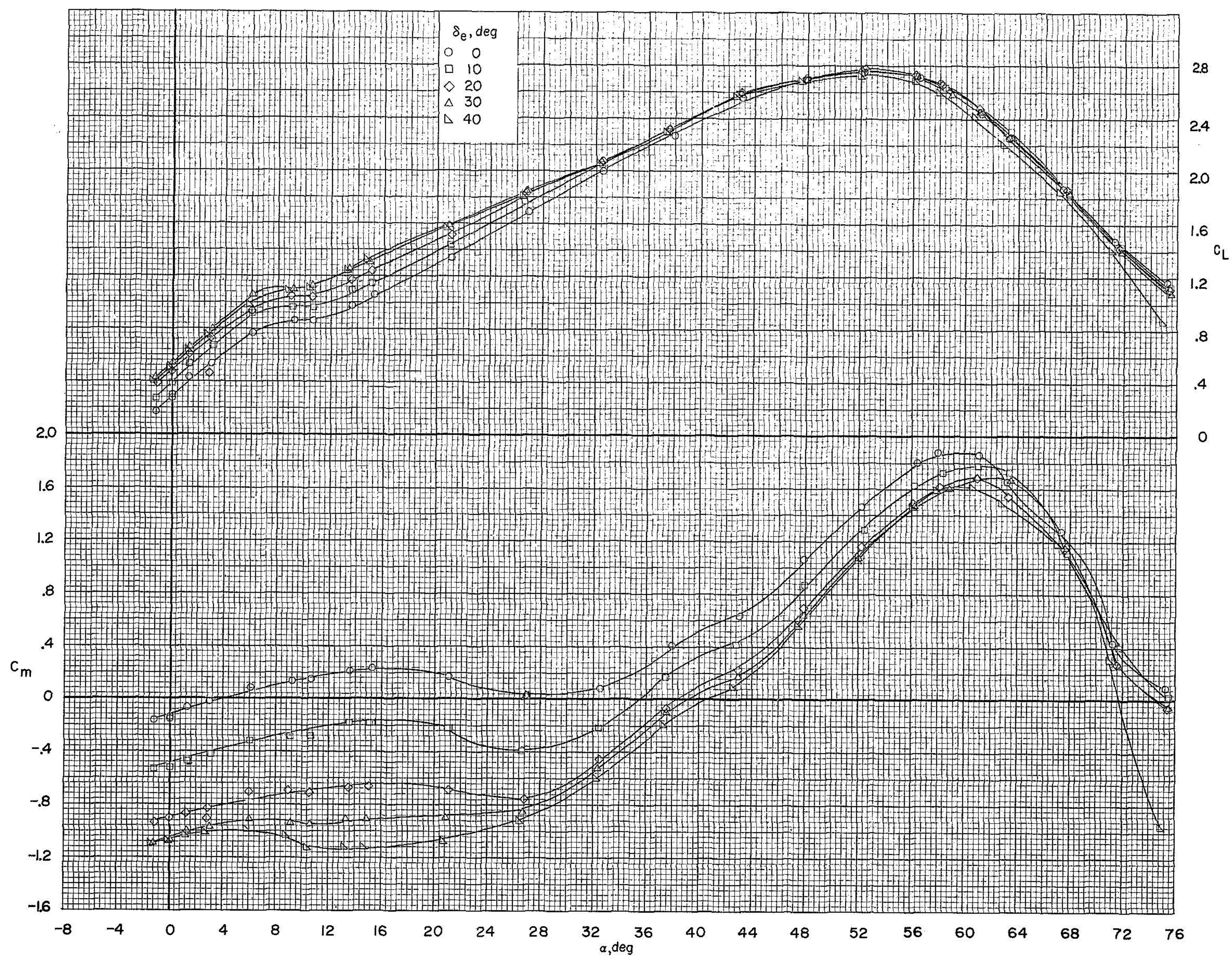

Figure 11.- Effect of positive elevator deflections on longitudinal aerodynamic characteristics of B_9WH_2V. $R/ft = 1.7 \times 10^6$ $(R/m = 5.6 \times 10^6)$.

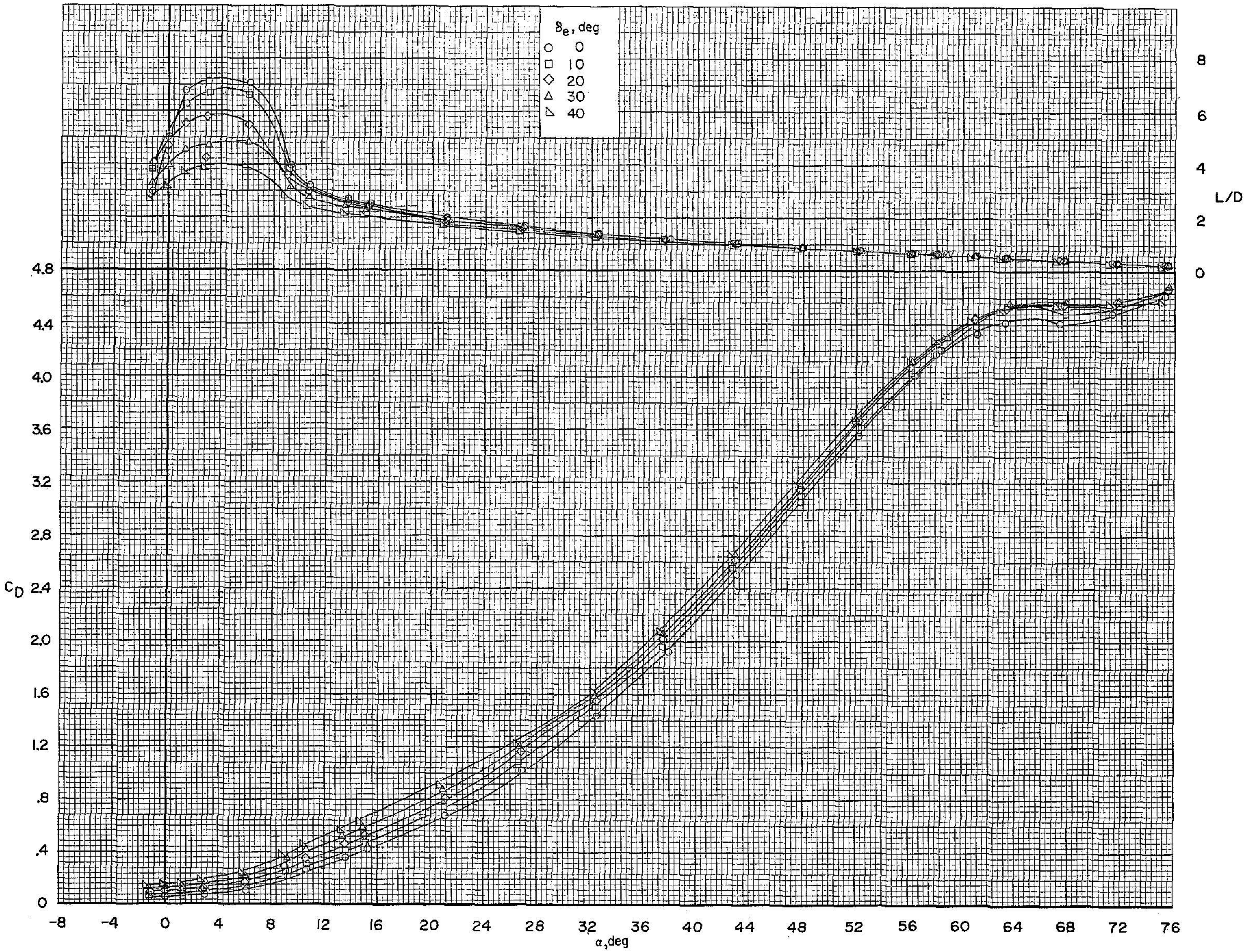

Figure 11.- Concluded.

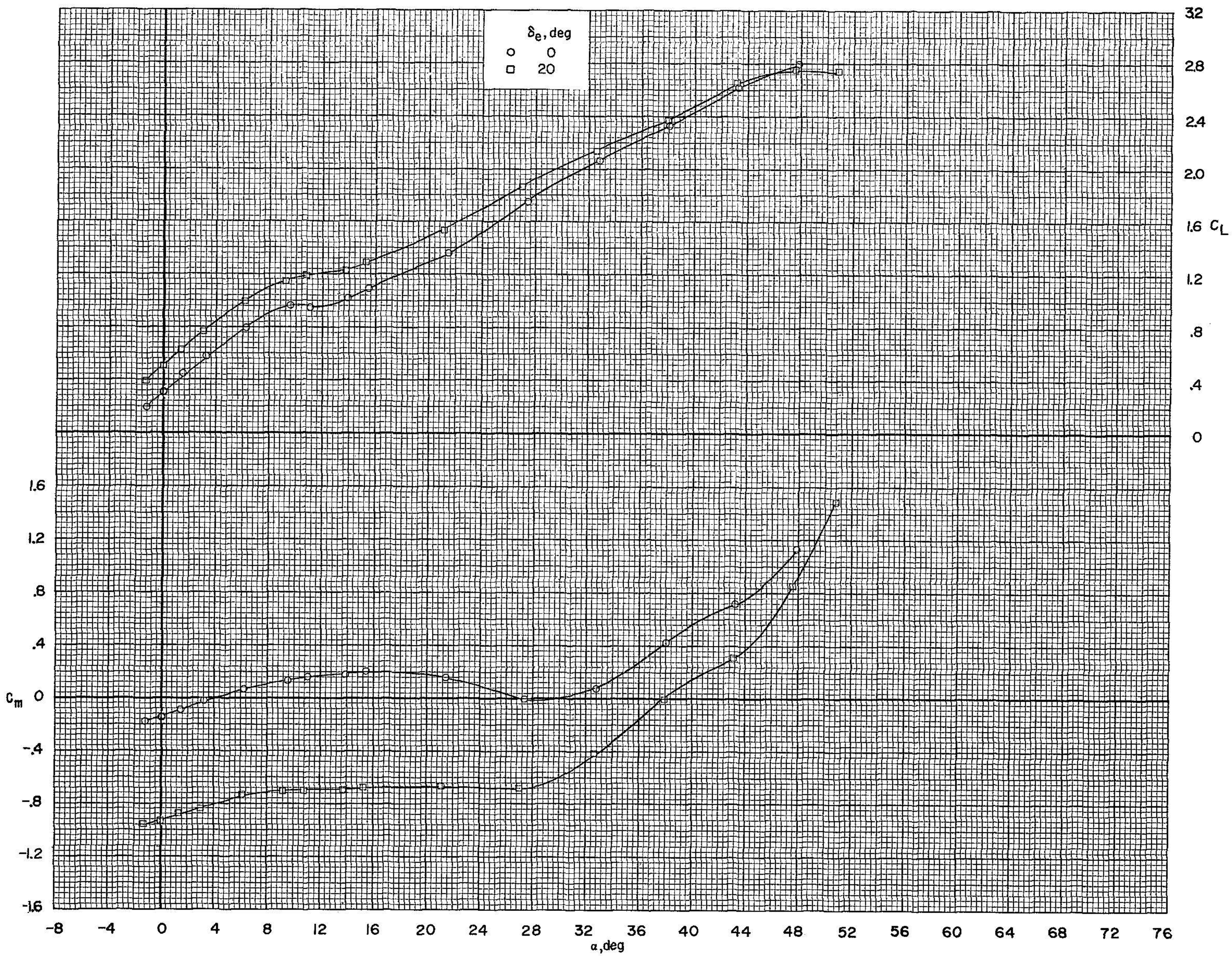

Figure 12.- Effect of positive elevator deflections on longitudinal aerodynamic characteristics of B_9WH_2V. R/ft = 3.2×10^6 (R/m = 10.5×10^6).

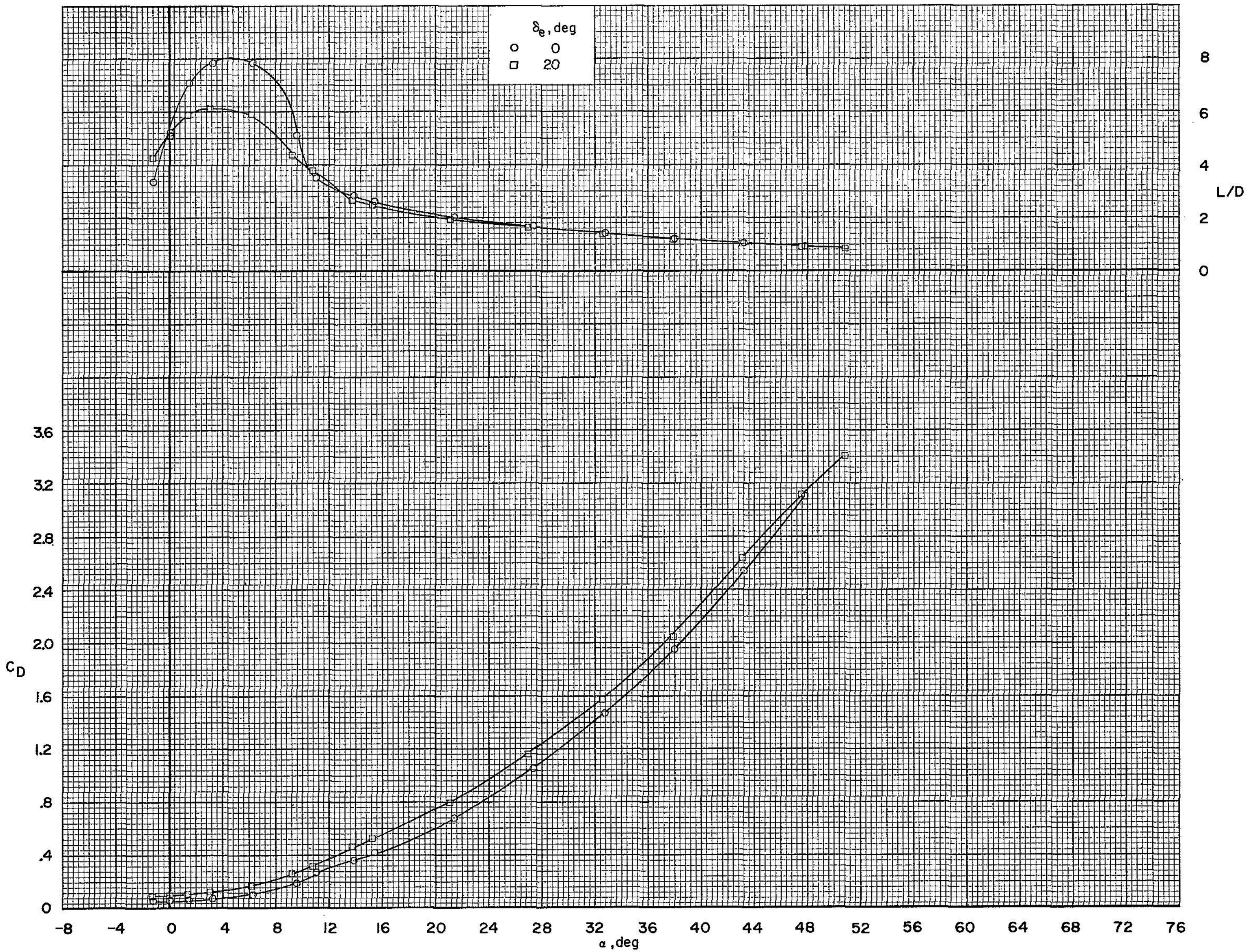

Figure 12.- Concluded.

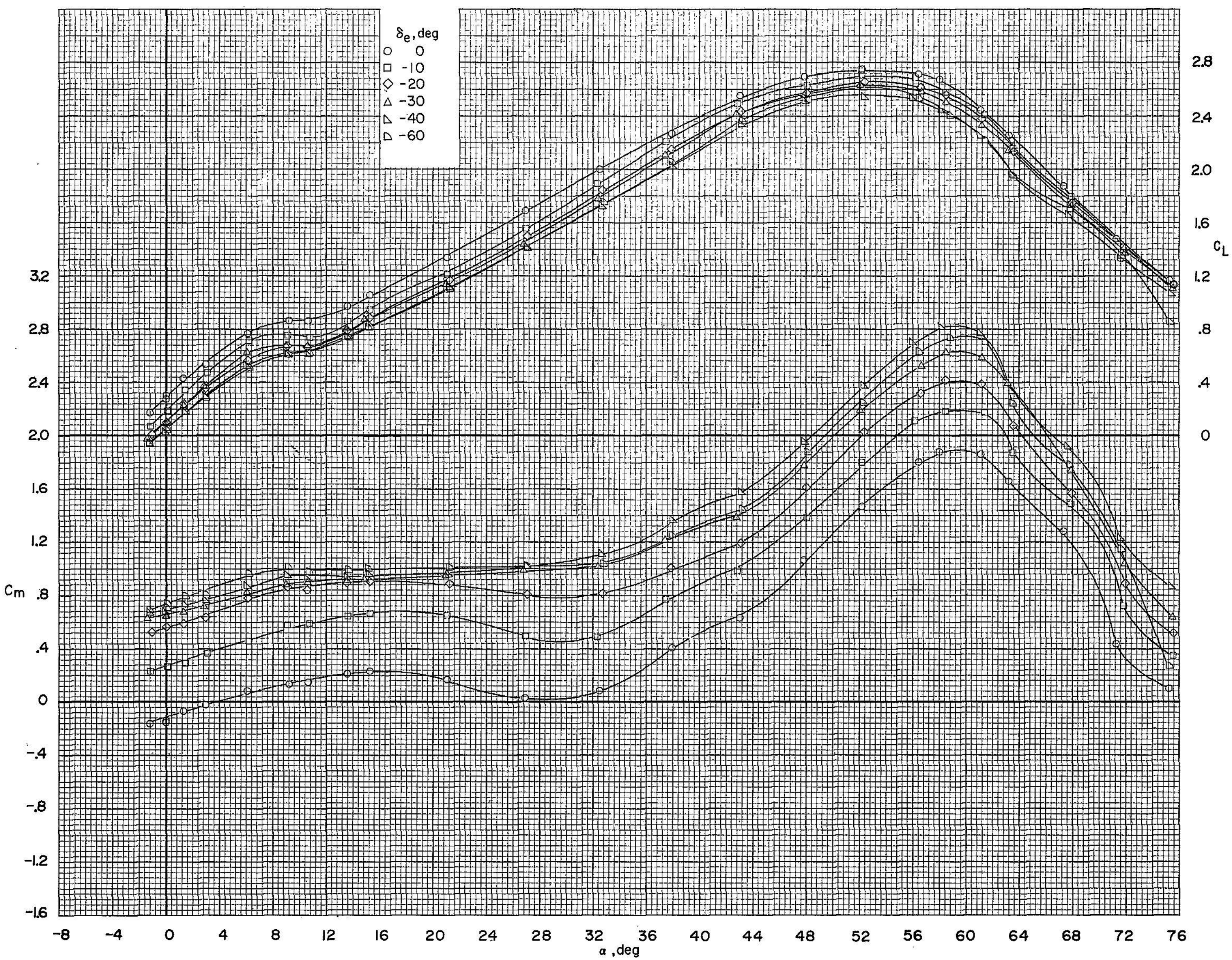

Figure 13.- Effect of negative elevator deflections on longitudinal aerodynamic characteristics of B_9WH_2V. $R/ft = 1.7 \times 10^6$ $(R/m = 5.6 \times 10^6)$.

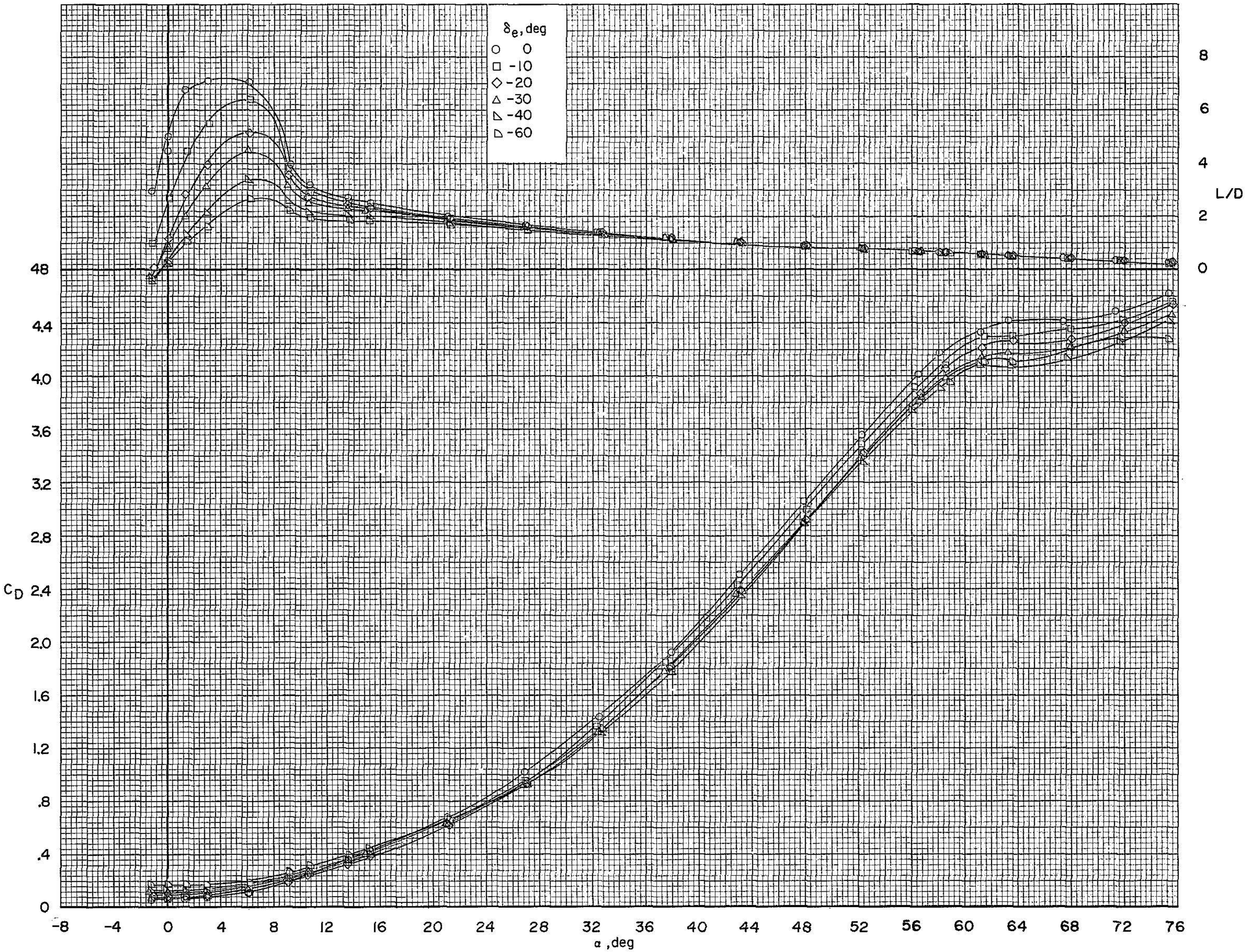

Figure 13.- Concluded.

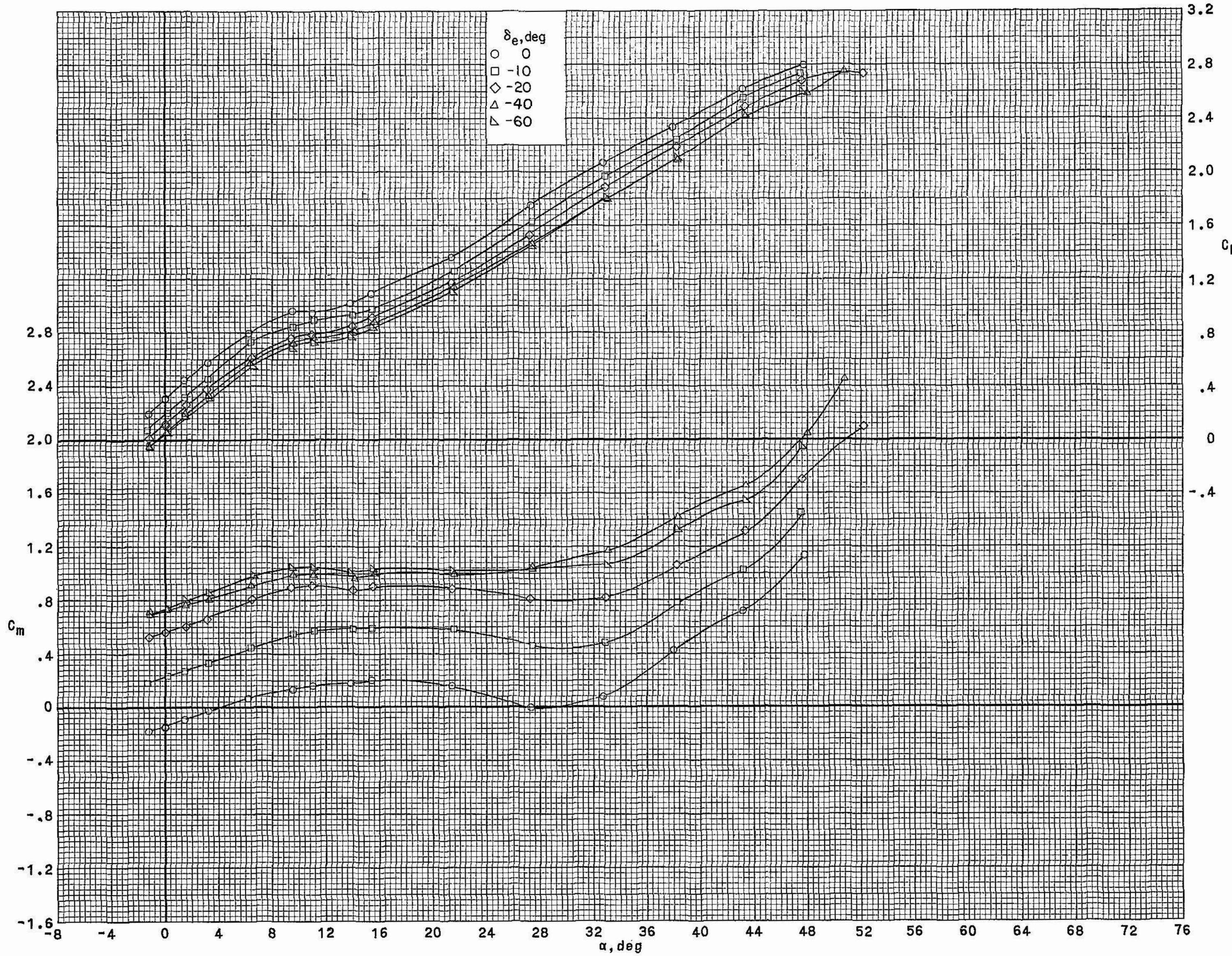

Figure 14.- Effect of negative elevator deflections on longitudinal aerodynamic characteristics of B_9WH_2V. R/ft = 3.2 × 10^6 (R/m = 10.5 × 10^6).

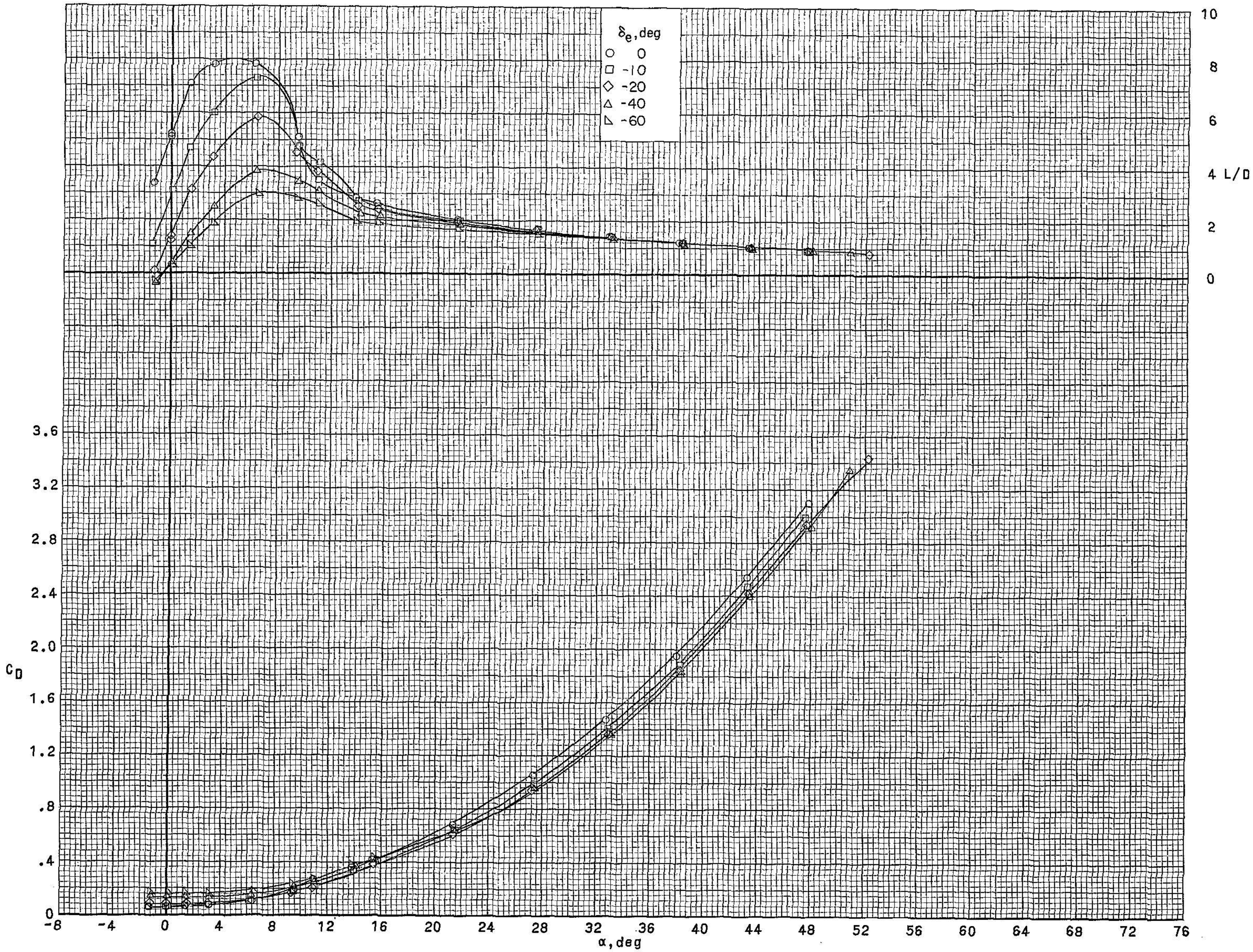

Figure 14.- Concluded.

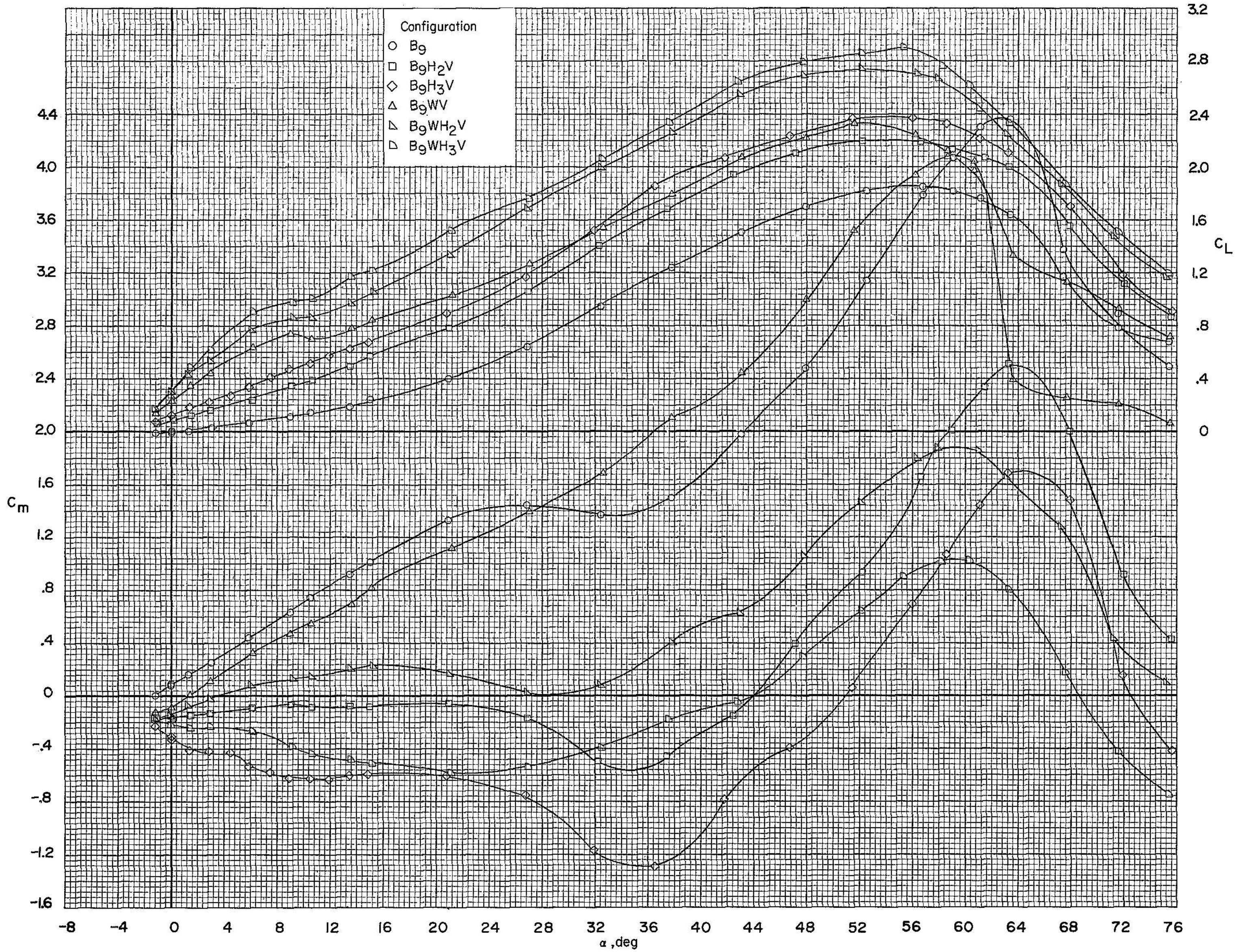

Figure 15.- Effect of various model components on longitudinal aerodynamic characteristics of B_9. $\delta_e = 0^0$; $R/ft = 1.7 \times 10^6$ $(R/m = 5.6 \times 10^6)$.

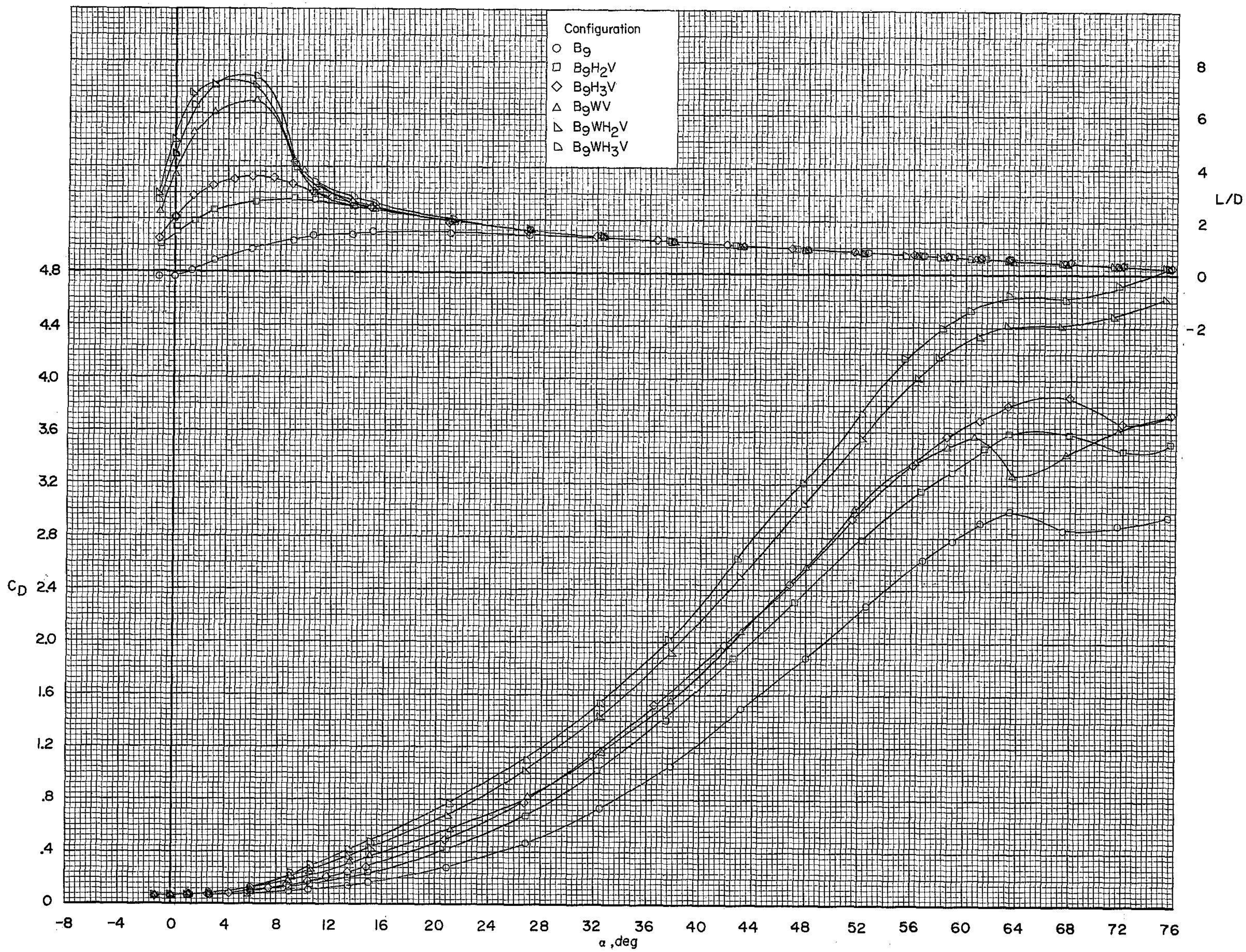

Figure 15.- Concluded.

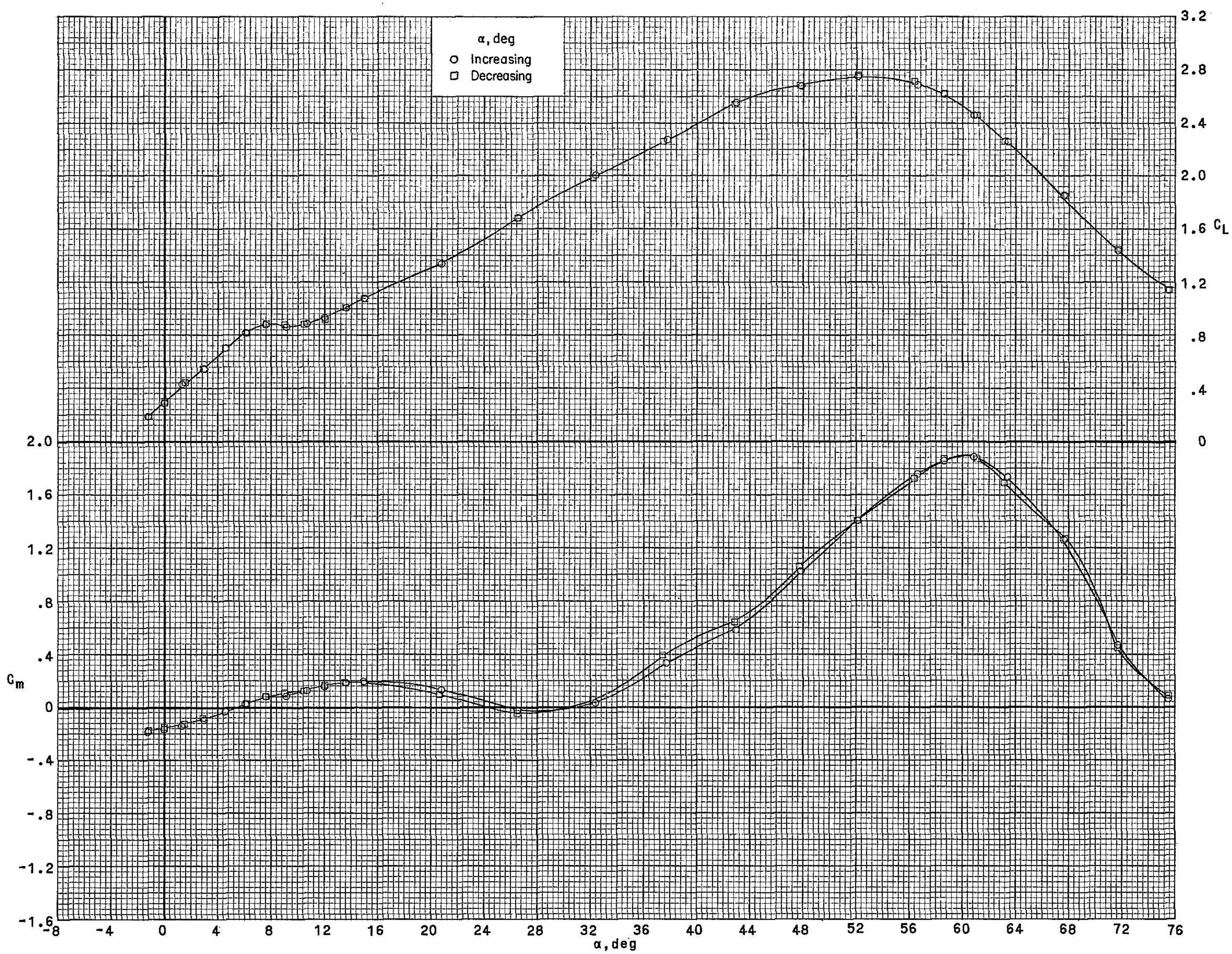

Figure 16.- Hysteresis effects on longitudinal aerodynamic characteristics of B_9WH_2V. $\delta_e = 0^o$; R/ft = 1.7×10^6 (R/m = 5.6×10^6).

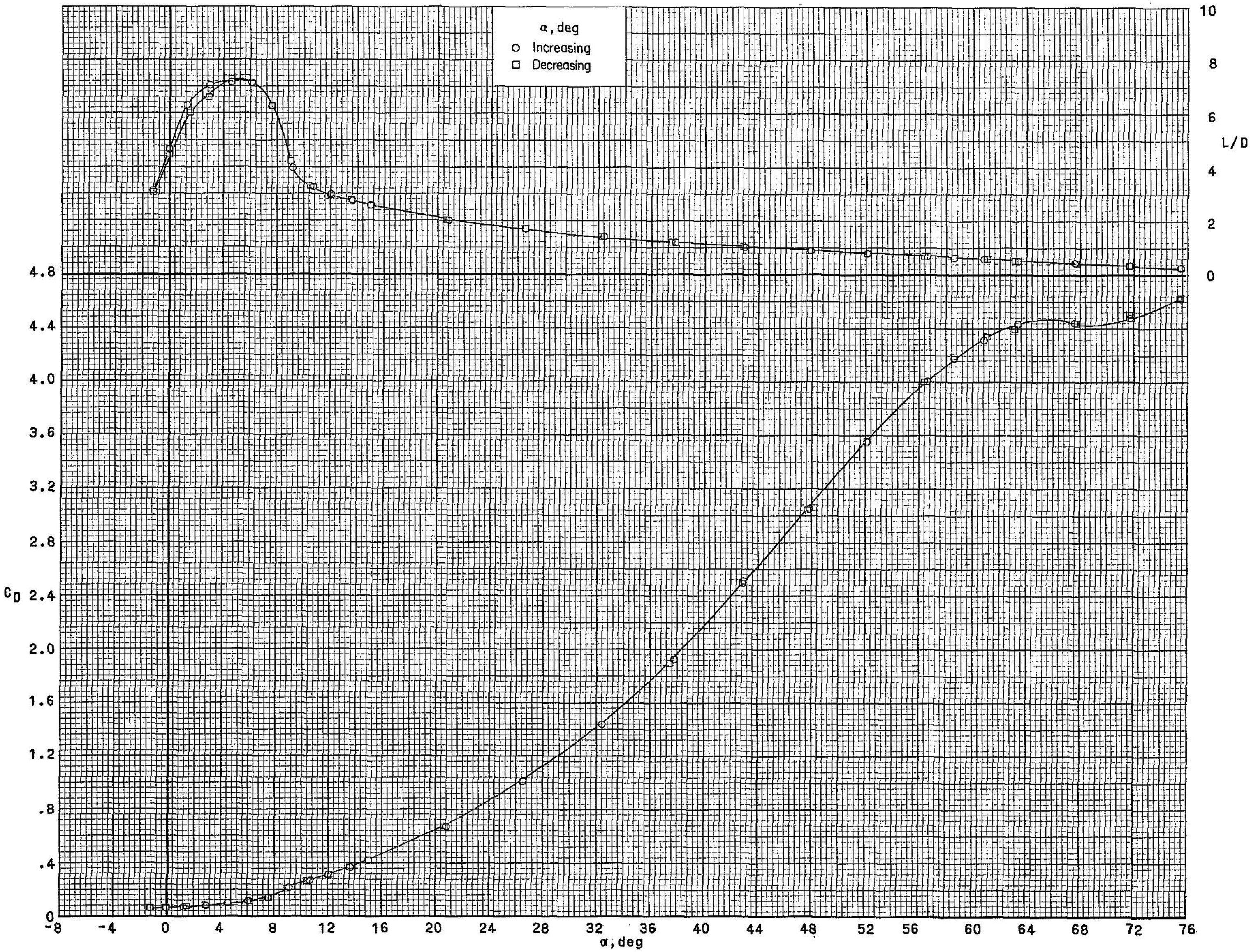

Figure 16.- Concluded.

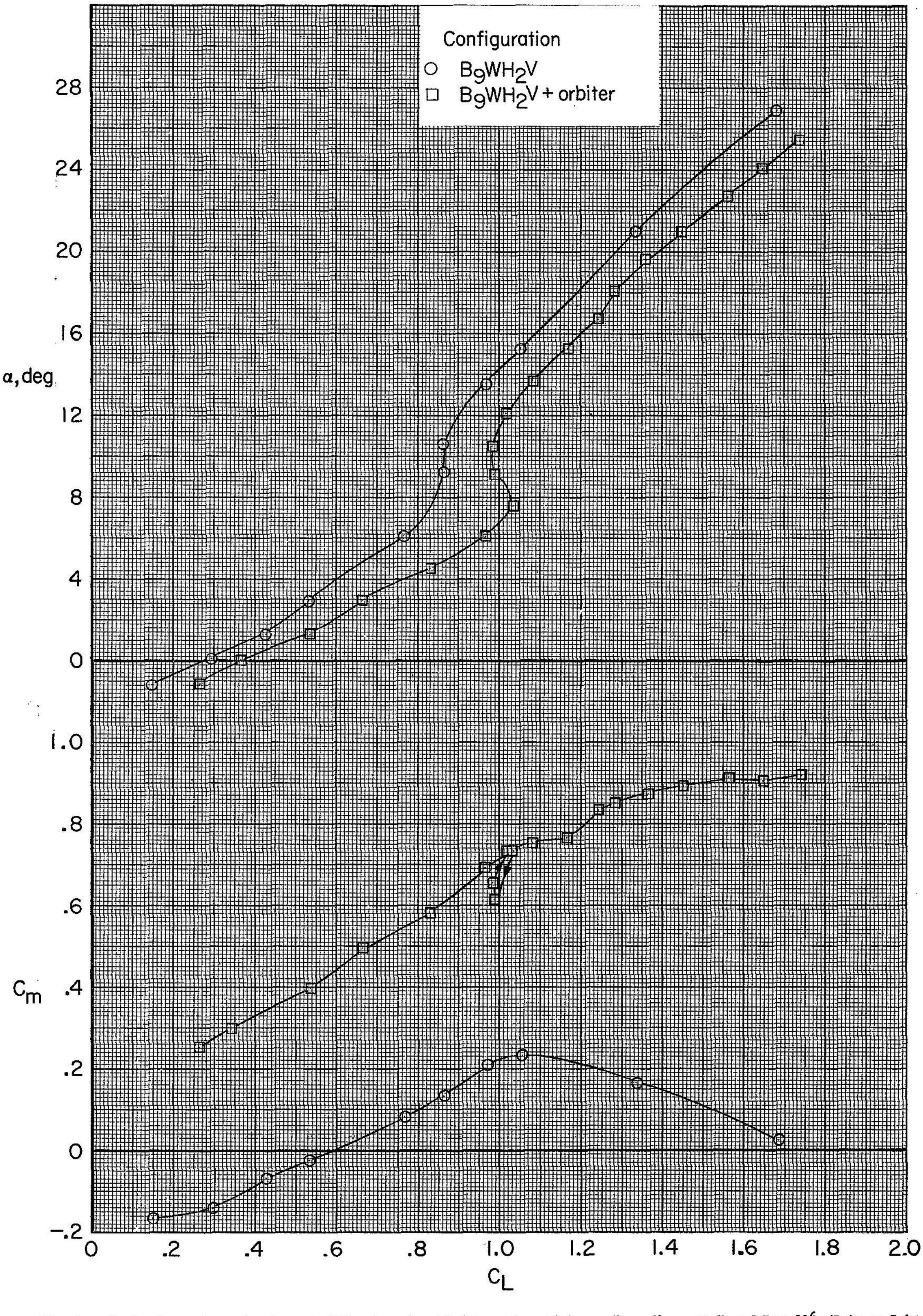

Figure 17.- Longitudinal aerodynamic characteristics for simulated launch-vehicle configuration. R/ft = 1.7×10^6 (R/m = 5.6×10^6).

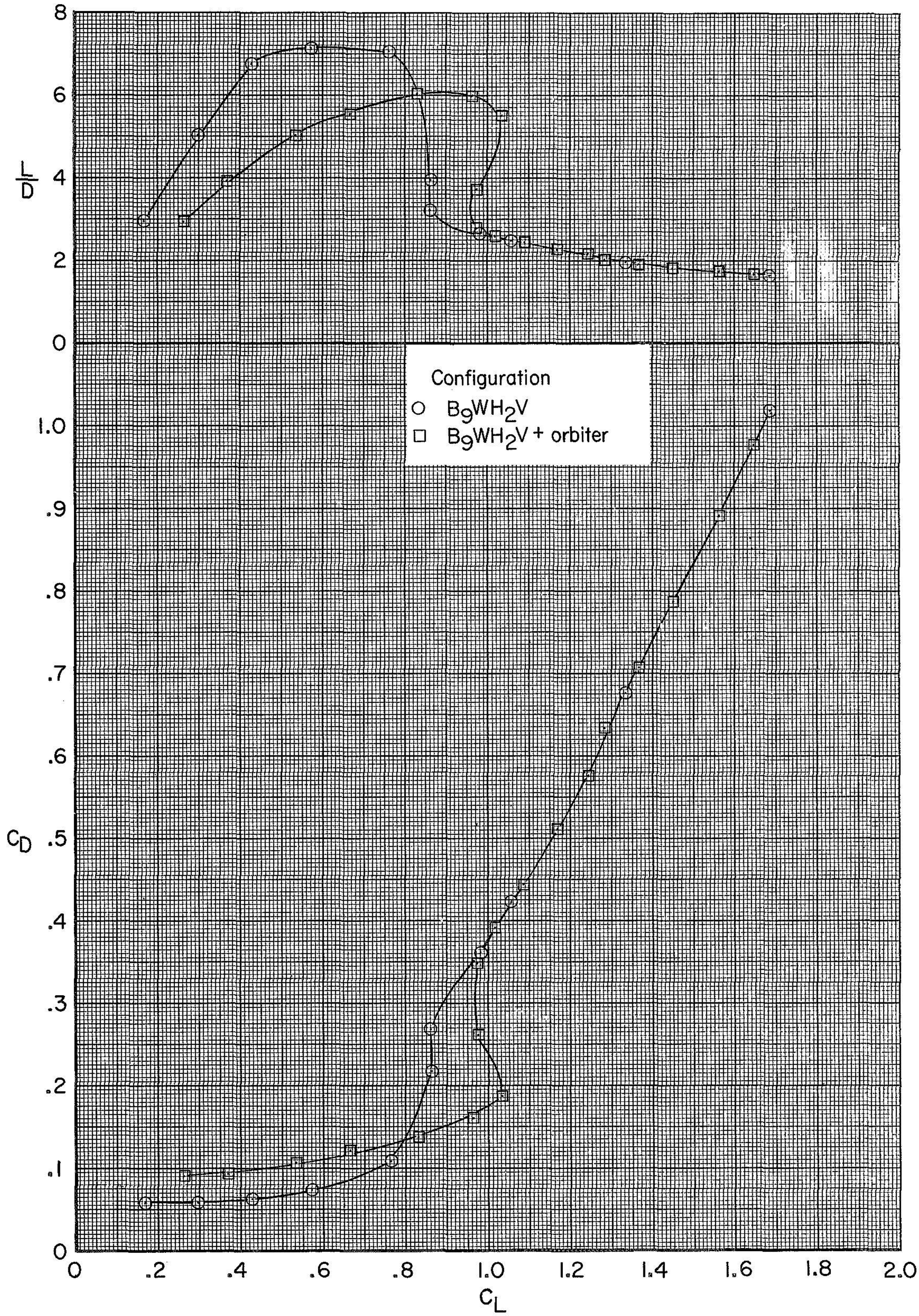

Figure 17.- Continued.

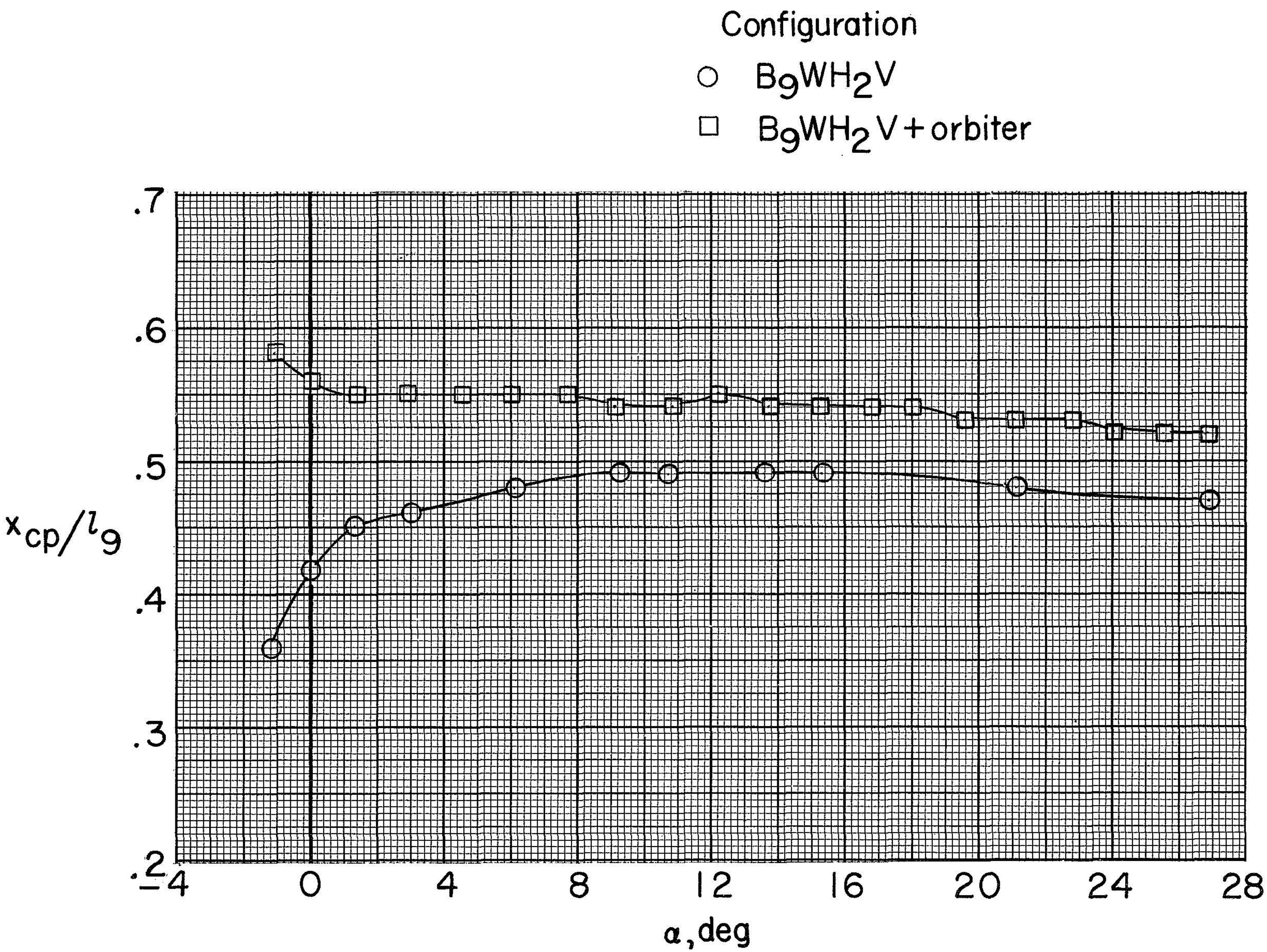

Figure 17.- Concluded.

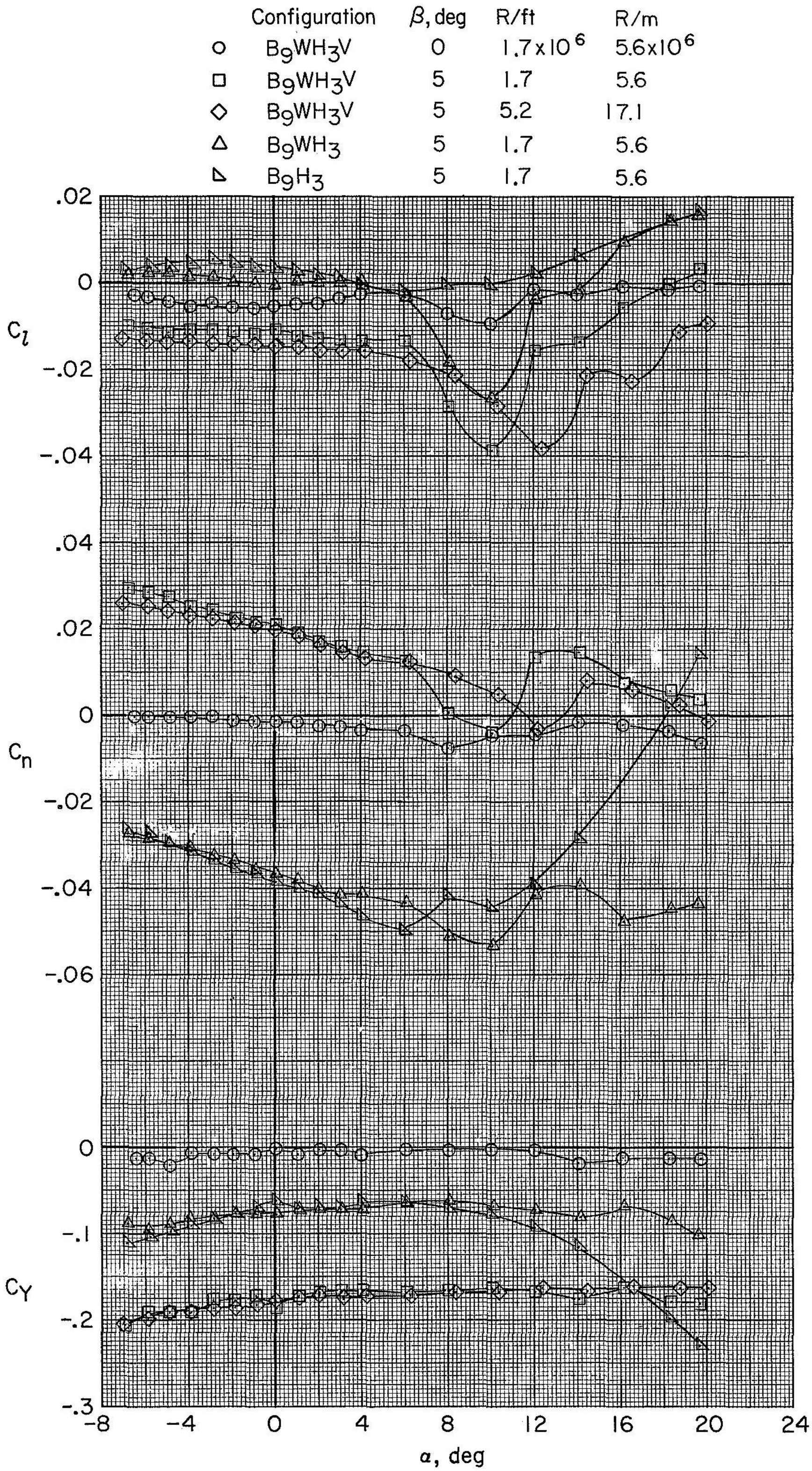

Figure 18.- Effect of various model components on lateral-directional aerodynamic characteristics. $\delta_e = 0^o$.

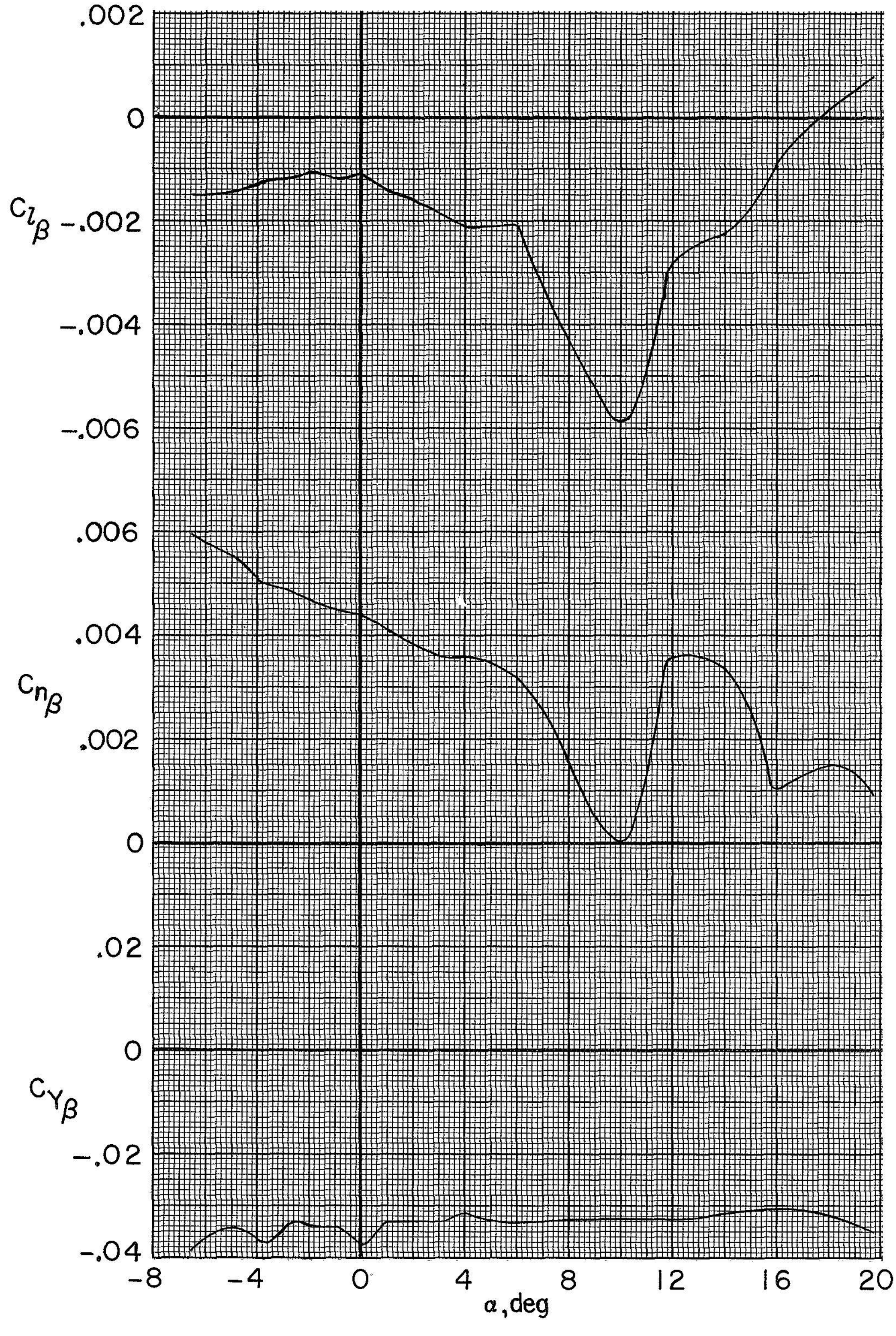

Figure 19.- Lateral-directional stability parameters for B9WH3V. $\delta_e = 0^\circ$; $R/ft = 1.7 \times 10^6$ $(R/m = 5.6 \times 10^6)$.

NASA-Langley, 1970 —— 1 L-6985

"The aeronautical and space activities of the United States shall be conducted so as to contribute . . . to the expansion of human knowledge of phenomena in the atmosphere and space. The Administration shall provide for the widest practicable and appropriate dissemination of information concerning its activities and the results thereof."

—NATIONAL AERONAUTICS AND SPACE ACT OF 1958

NASA SCIENTIFIC AND TECHNICAL PUBLICATIONS

TECHNICAL REPORTS: Scientific and technical information considered important, complete, and a lasting contribution to existing knowledge.

TECHNICAL NOTES: Information less broad in scope but nevertheless of importance as a contribution to existing knowledge.

TECHNICAL MEMORANDUMS: Information receiving limited distribution because of preliminary data, security classification, or other reasons.

CONTRACTOR REPORTS: Scientific and technical information generated under a NASA contract or grant and considered an important contribution to existing knowledge.

TECHNICAL TRANSLATIONS: Information published in a foreign language considered to merit NASA distribution in English.

SPECIAL PUBLICATIONS: Information derived from or of value to NASA activities. Publications include conference proceedings, monographs, data compilations, handbooks, sourcebooks, and special bibliographies.

TECHNOLOGY UTILIZATION PUBLICATIONS: Information on technology used by NASA that may be of particular interest in commercial and other non-aerospace applications. Publications include Tech Briefs, Technology Utilization Reports and Notes, and Technology Surveys.

Details on the availability of these publications may be obtained from:

SCIENTIFIC AND TECHNICAL INFORMATION DIVISION
NATIONAL AERONAUTICS AND SPACE ADMINISTRATION
Washington, D.C. 20546